Chapter II

Section B

Poly (methyl methacrylate)-graphene oxide supported palladium catalyst: A ligand free protocol for Suzuki and Heck coupling reaction in water medium

II.B.1. Introduction

Heterogeneous palladium catalyzed C-C cross coupling reactions have attracted much attention over past two decades. As a representative of this class of reaction, Suzuki and Heck coupling are most significant because biaryl moieties and substituted olefins are present in pharmaceuticals [1-4], wide range of natural products such as alkaloids and many agrochemicals and biologically active compounds [5,6]. Although homogeneous catalyst offers excellent result but they have some drawbacks because of difficult separation procedure often contaminates the products. However, most of them employ different types of ligands such as sterically hindered trialkyl phosphines, triarylphosphines [7], *N*-heterocyclic carbenes [8], based Pd (II) complexes. Use of these ligands is unenviable because they are toxic and moisture sensitive. However, with growing interest towards greener reactions, ligand free solid supported heterogeneous catalysts are in demand. They have the advantage of enhanced synthetic efficiency and operational simplicity [9-12]. Previous reports include the immobilization of Pd on activated carbon [13], polymers [14,15], zeolites [16], mesoporous carbon [17], silica, alumina or titania [18,19].

II.B.2. Background and objectives

In the recent years, graphene oxide (GO) has attracted much attention owing to its wide range of application in different fields such as fuel cells [20], nanocomposite materials [21-24], and electronic devices [25]. GO has two dimensional layered sheets with several oxygen containing functional groups like epoxy, hydroxy, carbonyl, carboxyl, etc. Palladium nanoparticles supported on graphene and graphene derivatives enlarge the surface area of the composite [26], increasing the distance between the sheets.

Scheuermann *et al.* employed PdNPs supported on chemically derived graphene (CDG) for Suzuki coupling reaction (Scheme II.B.1) [27]. The CDG-Pd catalyst was prepared by the immobilization of Pd^{2+} ions through cation exchange on graphite oxide followed by chemical reduction. In comparison to the Pd/C catalyst, garphene-based and graphite oxide based Pd catalyst showed higher catalytic activity due to low Pd leaching. The prepared catalyst was characterized by different spectroscopic techniques such as FTIR, AAS, XPS, solid state ^{13}C NMR.

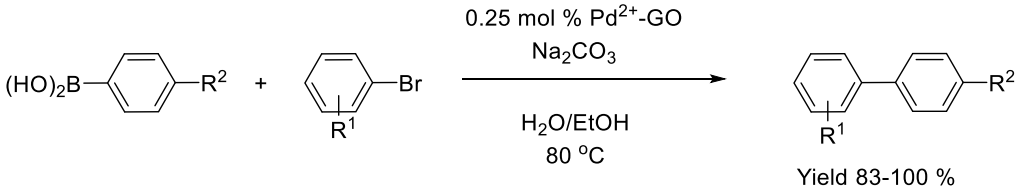

R^1= 4-OH, 3-OH, 4-OMe, 3-OMe, 4-CN, 4-CO_2H,4-CO_2Et, 4-NO_2, 3-CHO, heterocycle
R^2= OMe, H

Scheme II.B.1. *Chemically derived graphene (CDG)-Pd catalyzed Suzuki coupling reaction.*

Nagarkar *et al.* synthesized electrochemically deposited reduced graphene oxide and Pd catalyst (ERGO-Pd) for the efficient Suzuki and Heck C-C cross coupling reaction (Scheme II.B.2) [25]. The use of homogeneous palladium complexes has been restricted due to the problem of separation and their instability at elevated temperature. To overcome these major drawbacks, they developed a new GO-based heterogeneous catalyst and employed it in Suzuki and Heck reaction. They optimized the Suzuki coupling between aryl iodides/bromides and aryl boronic acids using K_2CO_3 base in ethanol solvent under refluxed condition. Whereas the optimized condition for the Heck reaction was achieved in DMF solvent in presence of Et_3N base at 120 ^oC temperature.

The high catalytic activity of ERGO-Pd in Suzuki and Heck reaction, attributed to the high dispersion of palladium NPs (PdNPs) on the ERGO support.

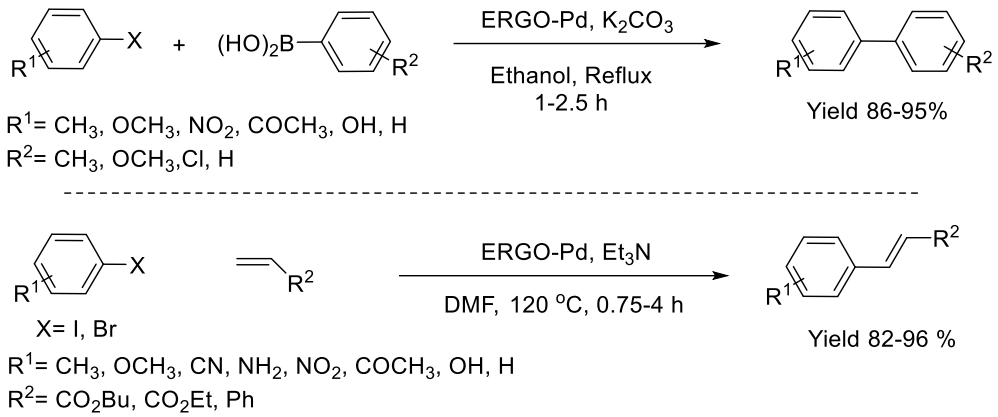

Scheme II.B.2. *Suzuki and Heck cross coupling reaction catalyzed by ERGO-Pd catalyst.*

In 2013, Kim *et al.* described the synthesis of the noble metal-graphene nanocomposites by reducing both noble metal and GO in hot water using ascorbic acid as reductant under hydrazine-free and surfactant free condition (Scheme II.B.3) [28]. During the synthesis of noble metal-graphene composite containing Pd, Pt, Ag and Au metal nanoparticles, complete reduction of metal salts and graphene oxide has been carried out by this procedure. Amongst them, Pd-graphene nanocomposite was utilized to catalyze the Suzuki-Miyaura coupling reaction with excellent product yield using K_2CO_3 as base at 90 ^oC temperature in presence of DMF solvent. This catalyst was recycled for many times without significant loss of the catalytic activity.

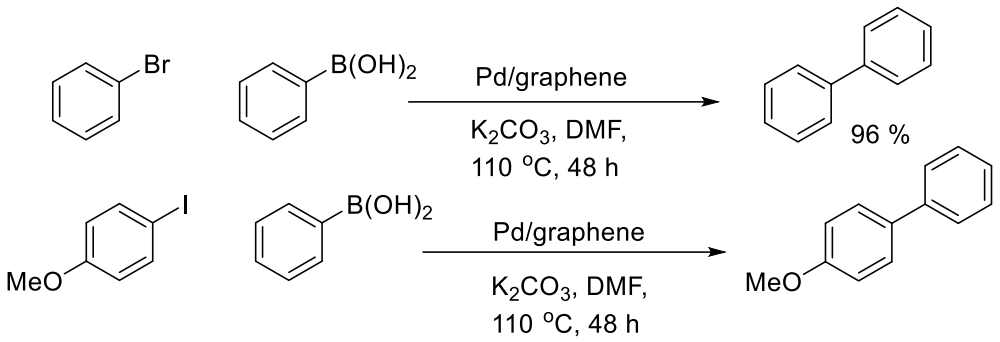

Scheme II.B.3. *Surfactant free Suzuki coupling reaction using Pd/graphene.*

In 2013, Nagarkar *et al.* synthesized Pd/nafion-graphene (Pd/Nf-G) catalyst from aqueous solution of Pd^{2+} ions by the electrochemical reduction followed by deposition on Nf-G support (Scheme II.B.4) [29]. The prepared catalyst was characterized by different spectroscopic techniques SEM, TEM, EDAX, XRD, TGA. The average size of the nanoparticle was maintained in the range of 4-12 nm. The high catalytic activity of this catalyst was observed for Suzuki coupling reaction using K_2CO_3 base, ethanol-water solvent at 80 °C temperature. This prepared catalyst was reused upto 5th cycle without loss of catalytic activity.

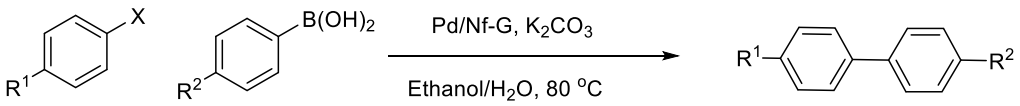

R^1= CH_3, OCH_3, NO_2, $COCH_3$, OH, H
R^2= CH_3, OCH_3, Cl, H
X= Cl, Br

Yield 88-95 %

Scheme II.B.4. *Synthesis of substituted biaryls using Pd/Nf-G catalyst.*

In 2014, Ghosh *et al.* described an efficient method for the synthesis of PdNPs supported on noncovalently functionalized graphene using 1-pyrene carboxylic acid (PCA-GNS-Pd). The catalytic activity of this novel PCA-GNS-Pd catalyst was observed in case of Suzuki and Heck cross coupling reaction in

water medium (Scheme II.B.5) [30]. The catalyst is highly stable in water due to its amphiphilic nature and it can be easily recovered and recycled up to five consecutive cycles. The electron rich and electron poor bromoarenes and chloroarenes are more challenging substrates but they exerted good yield of the desire alkenes and biphenyls using this catalyst.

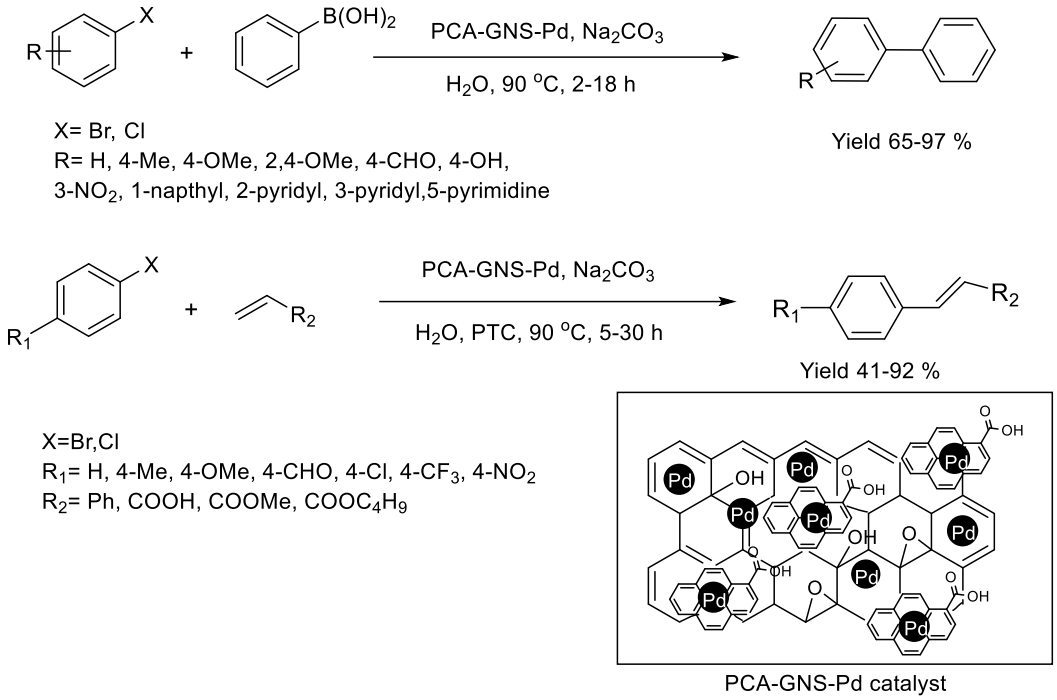

Scheme II.B.5. *Use of PCA-GNS-Pd catalyst in Suzuki and Heck coupling reaction.*

In 2016, Jain *et al.* designed a nanocomposite catalyst where PdNPs are dispersed on GO which is chemically modified with bidentate ligand containing N and S atoms (Scheme II.B.6) [31]. This synthesized graphene-ligand Pd complex (GL-Pd) with low weight % of Pd displayed excellent catalytic activity in Heck reaction between acrylates and arylhalides in presence of DMF/water solvent at 120 ^{o}C temperature. The structural analysis of GL-Pd hybrid was carried out using different spectroscopic techniques such as PXRD, FTIR,

Raman, XPS, SEM, TEM. The important feature of this prepared catalyst is its dispersibility in organic solvents which enables it to work effectively with a wide substrate scope.

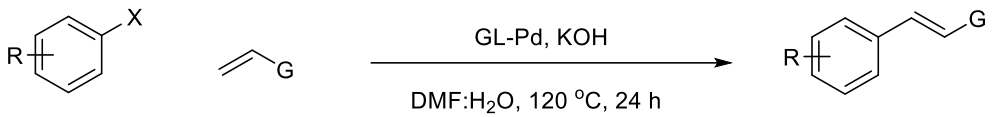

X= I, Br
R= H, 4-OMe, 2-OMe, 2-Me, 3-Me, 4-OAc, 4-CN
G= C_6H_5, 4-FC_6H_4, 4-*t*BuC_6H_4, 1-napthyl, 2-napthyl, CN, CO_2Me, CO_2Bu

Yield 73-97 %

Scheme II.B.6. *Suzuki coupling reaction catalyzed by GL-Pd hybrid catalyst.*

In 2018, Chen *et al.* discovered a biogenic method for the synthesis of PdNP modified reduced graphene oxide by using Ficus carica fruit juice as the efficient reducing agent. The catalyst PdNP/rGO has been applied as effective catalyst for Suzuki coupling reaction under both aerobic and aqueous condition (Scheme II.B.7) [32]. The catalyst was characterized by UV-Vis spectroscopy, Raman spectroscopy, XRD, TEM and FT-IR spectroscopy. The experimental results supported the spherical shape of PdNP/rGO and the dimension was estimated nearly 0.16 nm.

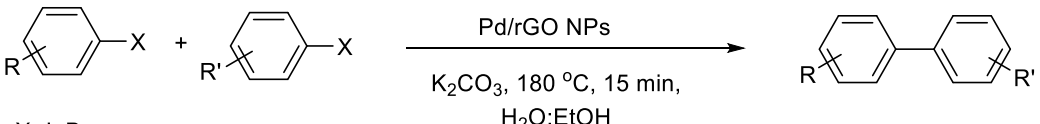

X- I, Br
R= H, 4-NO_2,4-CN, 4-OCH_3
R'= 2-CN, 3-Cl, 2,6-OCH_3, 3,4,5-OCH_3, 2,4-Cl

Yield 90-97 %

Scheme II.B.7. *PdNP/rGO for the synthesis of substituted biaryls.*

In 2020, Elhamifar *et al.* designed chemically modified graphene oxide supported Pd catalyst, through the coordination between $PdCl_2$ and 1,2-bis(4-aminophenylthio) ethane ligand (N_2S_2) which was grafted on the surface of GO

covalently (Scheme II.B.8). The catalytic activity of this prepared catalyst was observed in Suzuki coupling reaction between aryl halides and phenylboronic acids in presence of base K_2CO_3 in ethanol solvent [33]. This heterogeneous catalyst was characterized using different techniques XRD, FTIR, Raman, TEM, TGA. The catalyst was highly stable under reaction condition, recovered easily and reused upto several cycle without leaching of the active metal species.

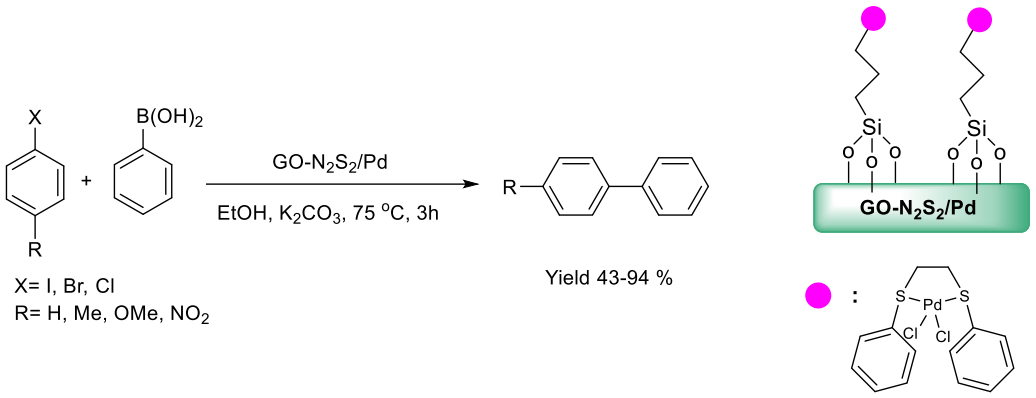

Scheme II.B.8. *GO-N_2S_2/Pd catalyzed Suzuki cross coupling reaction.*

II.B.3. Present Work: Result and Discussion

Preliminary studies on polymer supported GO has revealed significant increase in mechanical and thermal properties of the composite [34-37]. Driven by this fact, the idea of a new solid support automatically comes which allows better stability, easy recovery of products and simple separation procedure. Poly (methyl methacrylate) [PMMA] is a nonconductive polymer and its composite with GO enhances the thermal stability of the material. Based on the above perspective, our present explorative work involves the deposition of Pd NPs on GO-PMMA composite via in situ polymerization of MMA. Wielded by the environmental concern, water is selected as solvent instead of hazardous solvents such as DMF, DMA, NMP, etc. Utility of GO enhances the thermal

stability of poly (methyl methacrylate) [38, 39] and Pd NPs are strongly immobilized in between the layers of graphene oxide–PMMA composite [25, 29]. To the best of our knowledge, GO-PMMA supported Pd catalyst has not been employed in Suzuki and Heck coupling reactions (Scheme II.B.9). Simpler reaction conditions, ligand free protocol, low Pd content and tolerance to wide range of functional groups are the salient features of our work.

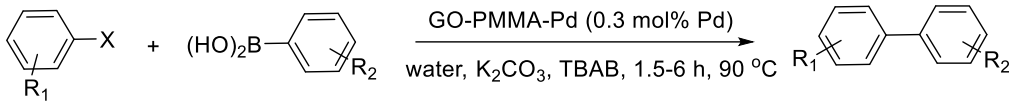

Yield (58-93 %)

R_1= 4-OMe, 3-OMe, 3-NO_2, 4-Me, 3-Me, 4-COMe, 4-OMe, Thienyl
R_2=H, 4-Me, 4-OMe, 3-NO_2
X= I, Br

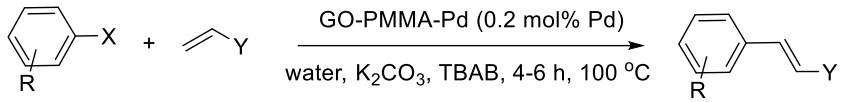

R= 4-OMe, 3-NO_2, 4-COMe
X= I, Br, Y= COOMe, COOEt, COOBu, Ph

Yield (79-90%)

Scheme II.B.9. *GO-PMMA-Pd(0) composite catalyzed Suzuki and Heck reaction.*

II.B.3.1. General procedure for preparation of GO-PMMA-supported Pd catalyst

Initially for the preparation of catalyst 20 mg of GO was suspended in 20 mL of toluene. The slurry was then dispersed through ultrasonication for 60 min. After ultrasonication methyl methacrylate was injected to well dispersed solution of GO. Benzoyl peroxide (BZP, 0.1 mol%) was added to initiate the polymerization of methyl methacrylate (MMA). The resulting mixture was then

stirred well at 90 ºC for 4 h. The temp of the solution was maintained at 90 ºC. Stirring was continued for another 3 h followed by the addition of 40 mg $Pd(OAc)_2$ and 100 mg of HCOOH as shown in Scheme II.B.10. The dark brown precipitate instantly turned into black after the addition of HCOOH. The obtained residue was washed several times with water and residual solvent was shuffled off by rotary evaporator, and dried at 60 ºC.

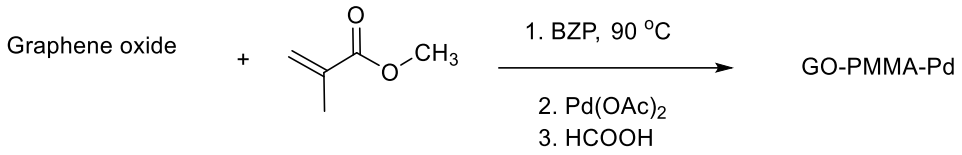

Scheme.II.B.10. *GO-PMM Preparation of GO-PMMA-Pd catalyst.*

II.B.3.2. Characterisation of GO-PMMA-Pd catalyst

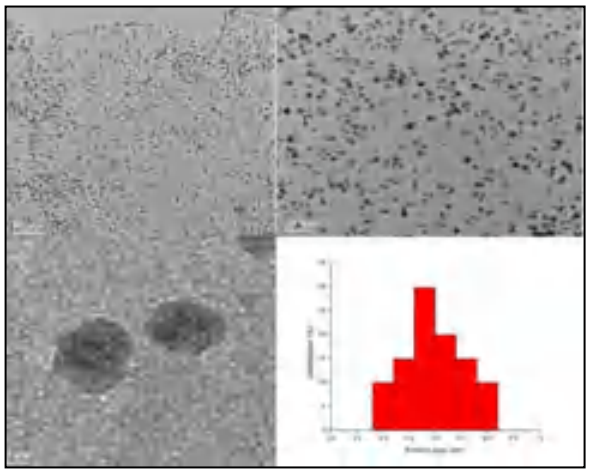

Figure II.B.1. *TEM image of GO-PMMA-Pd composite catalyst (a) at 50 nm (b) at 20 nm (c) at 2 nm (d) Particle size distribution curve of GO-PMMA-Pd catalyst.*

The morphology of the catalyst (GO-PMMA-Pd) was analyzed by Transmission Electron Microscope. The micrograph and particle size distribution curve of in situ prepared GO-PMMA-Pd catalyst is represented in Figure II.B.1. The TEM images show the mono dispersed palladium without agglomeration on the GO-PMMA-sheet during in situ polymerisation of MMA. The average size of the Pd NPs has been determined from the TEM images and was found to be around 4.8 nm.

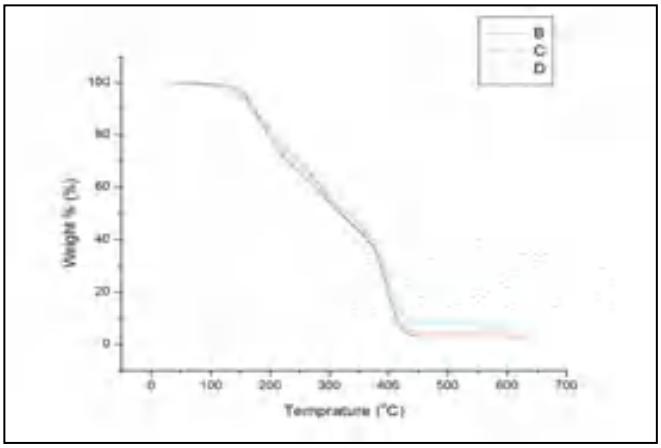

Figure II.B.2. *TGA results of (B) 2wt% (C) 5wt% (D) 10wt% GO in PMMA.*

The catalyst life is a factor that can control the economic viability of industrial processes and as a consequence high thermal resistance of a catalyst support is found to be suitable for different kinds of thermal reaction [40]. In view of the above, thermogravimetric Analysis (TGA) of the solid support has been analyzed for several samples with different wt % of GO loading as shown in Figure II.B.2. It is very interesting to observe that composite with the lowest wt % of GO exhibited maximum thermal stability (Figure II.B.2.).

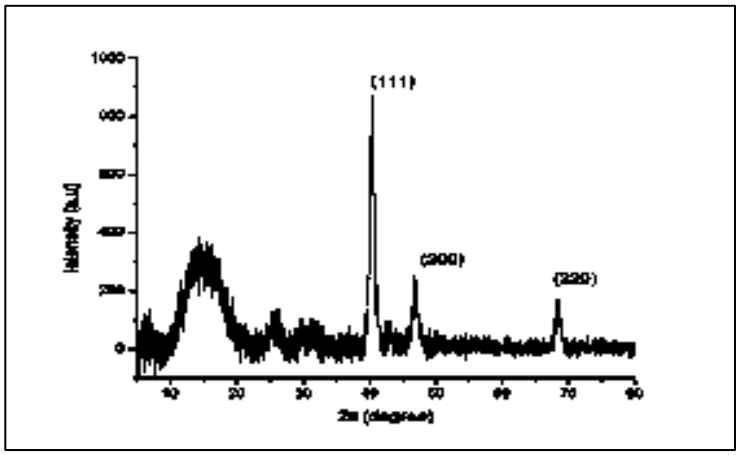

Figure II.B.3. *XRD pattern of GO-PMMA-Pd composite catalyst.*

The catalyst was subjected to powder X-ray diffraction (XRD) for composition analysis (Figure II.B.3). Three sharp peaks at around 2Θ 40.1°, 46.6° and 68.9° represents the crystalline planes (111), (200) and (220) respectively in fcc structure of Pd [38]. However the intensity of (111) plane is higher than (200) and (220) plane. The absence of strong GO peak at 2Θ= 10.63° [41] and the appearance of characteristic broad PMMA peak at 2Θ= 14.8° indicated the formation of GO-polymer composite. The FTIR spectrum of GO has a peak at 1735 cm^{-1} which is assigned to the carbonyl stretching frequency. The FT-IR peak of PMMA at 1148 cm^{-1} is associated with the stretching vibration of the C-O bond in the C-O-C moiety whereas the peak at 1731 cm^{-1} is due to the acrylate carbonyl groups. FT-IR spectrum (Figure II.B.4) revealed that the resultant GO-PMMA-Pd composite catalyst contained several functional groups like –OH (3454 cm^{-1}) and C=O (1731 cm^{-1}). Therefore, it has a strong tendency to readily interact with metal ions by hydroxyl and carboxyl group.

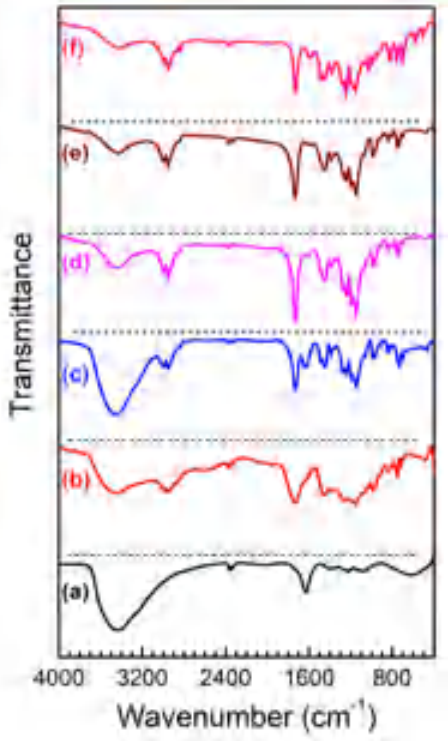

Figure II.B.4. *Comparison of FT-IR spectra of (a) GO (b) GO-PMMA (c) GO-PMMA-Pd (d) PMMA-Pd (e) PMMA and (f) recycled catalyst after fifth run.*

It is considered that the bond between Pd and GO-PMMA can be formed through some physical / chemical interactions such as Vander Waals force, H-bonding and other bonds [42]. The shift of other stretching frequencies also points towards the association of PMMA with GO (Figure II.B.4). Furthermore, a hump obtained at around $2\Theta = 23^{o}$ suggests the presence of reduced graphene oxide (rGO) (Figure II. B.3) [43]. Hence, it can be concluded that a small amount of GO has been converted into rGO when HCOOH was employed. GO-PMMA-Pd catalyst was further characterized by XPS, as shown in Figure II.B.5. High-resolution XPS spectrum was corrected with reference to the carbon 1s peak at 284.8 eV shown in figure 5 (b). The binding energies of Pd 3d at 335.87

and 341.2 eV for GO-PMMA-Pd corresponded to the Pd^0 Pd $3d_{5/2}$ and Pd $3d_{3/2}$, respectively. Thus the presence of metallic Pd in the composite is confirmed [Figure II.B.5 (c)].

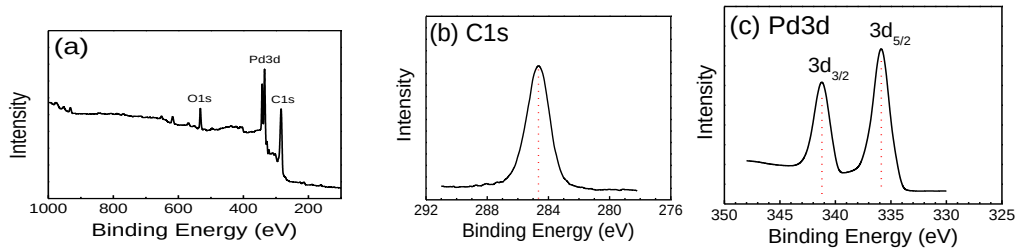

Figure II.B.5. *(a) Full-range XPS spectrum of GO-PMMA-Pd catalyst. C 1s peak at 284.8 eV shown in (b). In (c) the binding energies of Pd 3d at 335.87 and 341.2 eV for GO-PMMA-Pd corresponded to the Pd^0 Pd $3d_{5/2}$ and Pd $3d_{3/2}$, respectively.*

II.B.3.3. Catalytic activity of GO-PMMA-Pd catalyst in Suzuki and Heck cross coupling reaction

The development of recoverable catalyst is one of the indispensable principles of the green synthetic organic chemistry and the key purpose of this study was to place a recyclable catalyst for Suzuki and Heck reaction in aqueous medium. Initially, for screening the reaction, phenylboronic acid and 4-iodo anisole has been chosen as the model substrates in presence of GO-PMMA-Pd catalyst. The favorable condition of the reaction was achieved by varying the parameters such as catalyst loading, solvent, time, base and temperature. Finally the protocol was optimized by using water as solvent, K_2CO_3 as base and catalyst loading (0.3 mol % Pd) in 6 mg of GO-PMMA-Pd catalyst at 90 ^oC (Table II.B.1). In order to enhance the yield of 4-methoxy-1,1′ biphenyl in water,

different surfactants were employed in the study (Table II.B.1). It is established that the yield of the product can be improved by increasing the reaction time. We started increasing the reaction time by keeping all parameters similar and found that the best yield is achieved in 4 hrs of reaction (Table II.B.1, entry 6). However, ortho-substituted compounds require longer reaction time.

Table II.B.1. Optimization of reaction parameters for Suzuki reaction based on the result of the following combination in the protocol[a]

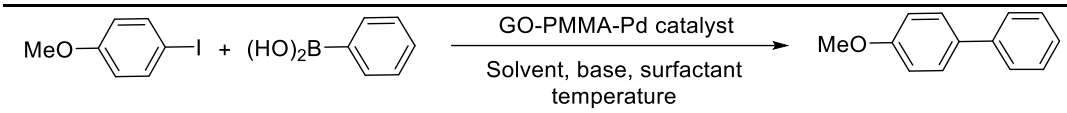

Entry	Solvent	Base	Pd loading (mol%)	Additive	Time (h)	Yield (%)[b]
1	DMF	K_2CO_3	0.1	Bu_4NBr	1	42
2	DMSO	K_2CO_3	0.1	Bu_4NBr	2	29
3	Water	K_2CO_3	0.2	Bu_4NBr	3	63
4	Ethanol	K_2CO_3	0.2	Bu_4NBr	3	58
5	Water	K_2CO_3	0.3	SDS	4	72
6	**Water**	**K_2CO_3**	**0.3**	**Bu_4NBr**	**4**	**90**
7	Water	Na_2CO_3	0.3	Bu_4NBr	6	76
8	Water	Cs_2CO_3	0.3	Bu_4NBr	6	75
9	Water	Et_3N	0.3	Bu_4NBr	6	78
10	Water	KOH	0.3	Bu_4NBr	4	62
11	Water	K_2CO_3	0.3	CTAB	6	72

12	Water	K_2CO_3	0.3	TMAI	4	52
13	Water	K_2CO_3	0.3	Bu_4NBr	24	25[c]
14	Water	K_2CO_3	0.5	Bu_4NBr	12	86[d]

[a]Reaction of 4-Iodo anisole (1 mmol), Phenyl boronic acid (1.5 mmol), Pd loading (0.3 mol%), K_2CO_3 (1 mmol), TBAB (10 mol%), water (2 mL) at 90 ^oC.

[b]Isolated yields.

[c] Room temperature reaction.

[d]Temp of the reaction 100 ^oC.

The synthetic efficacy of this catalyst in water mediated Suzuki coupling reaction was conducted with a number of different aryl halides and arylboronic acids under optimized condition. The electron withdrawing aryl iodides and bromides gave excellent yields of corresponding products. Although relatively longer reaction time was required for electron donating aryl iodides and bromides but each of them offered an excellent yield of products (Table II.B.2). The aryl chlorides gave only trace amount of the corresponding product even after 24 h of exertion of reaction (Table II.B.2, entry 14). The arylboronic acids with methoxy, methyl, nitro groups were rapidly converted to their corresponding products at high to moderate yield at 90 ^oC.

Table II.B.2. GO-PMMA-Pd catalyzed Suzuki reaction of different aryl halides with phenyl boronic acid[a]

Entry	Aryl halide	Boronic acid	Product	Time (h)	Yield (%)[b]

1	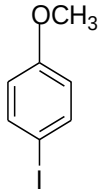	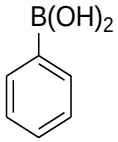	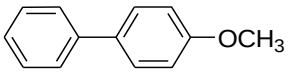	4	90
2	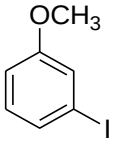	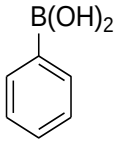	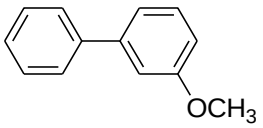	4	88
3	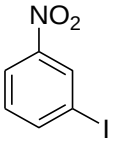	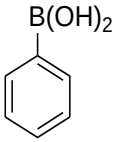	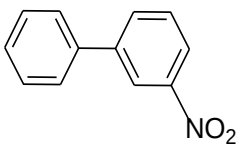	2	92
4	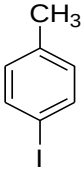	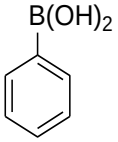	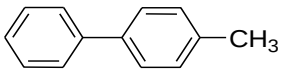	6	86
5	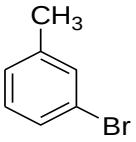	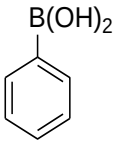	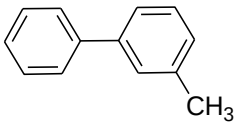	6	84
6	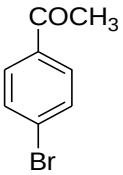	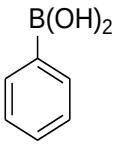	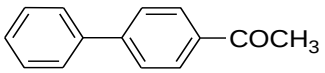	1.5	93

7	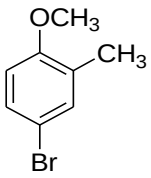	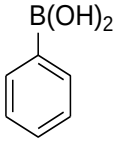	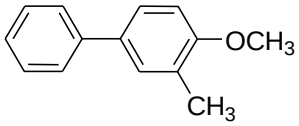	4	85
8	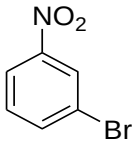	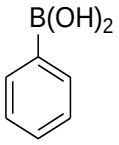	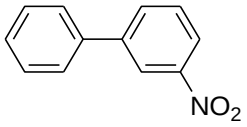	3	89
9	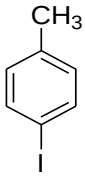	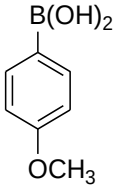	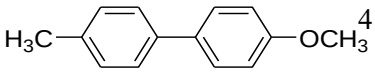	4	86
10	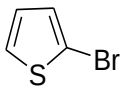	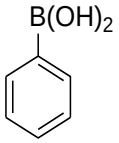	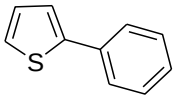	6	58
11	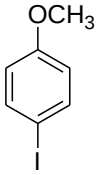	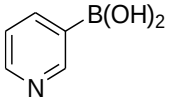	No reaction	-	Nil
12	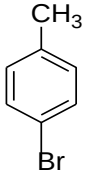	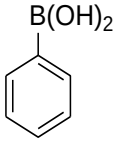	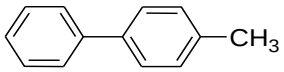	6	79

13	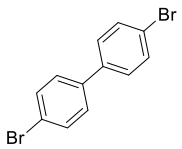	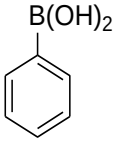	No reaction	-	Nil
14	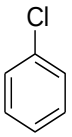	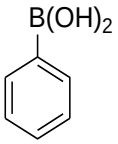	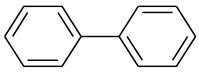	24	35[c]
15	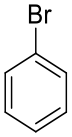	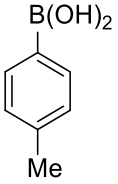	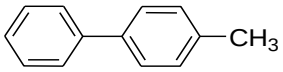	4	88
16	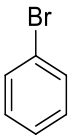	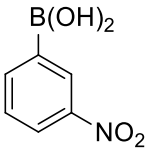	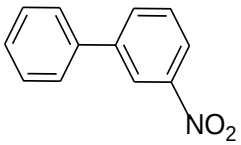	4	71

[a]Reaction of Aryl halide (1 mmol), Phenyl boronic acid (1.5 mmol), palladium loading (0.3 mol%), K_2CO_3 (1 mmol), TBAB (10 mol%), water (2 mL) at 90 °C.

[b]Isolated yields.

[c]Reaction temperature 120 °C

The above success in Suzuki coupling reaction prompted us to look for such expectancy in Heck coupling reaction too. The Heck reaction was optimized by varying the reaction parameters temperature, solvent, base, catalyst loading (Table II.B.3). In that instance, 4-iodo anisole was successfully coupled with methyl acrylate in presence of TBAB and 0.2 mol% Pd in GO-PMMA-Pd catalyst at 100 °C (Table II.B.3, entry 4). All types of aryl halides gave good to excellent yield which indicates the high efficiency of this heterogeneous catalyst (Table II.B.4) in Heck coupling too.

Table II.B.3. Optimization of reaction parameters of Heck reaction[a]

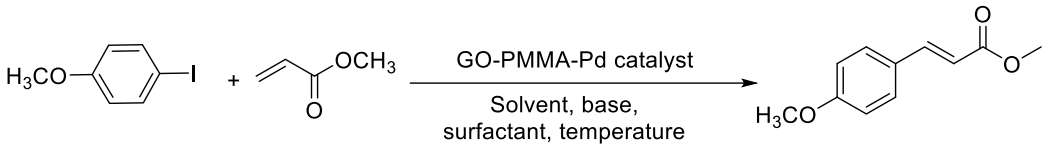

Entry	Solvent	Base	Temp (°C)	Pd-loading (mol%)	Time (h)	Yield(%)[b]
1	DMF	K_2CO_3	120	0.1	4	75[c]
2	Water	K_2CO_3	100	0.1	5	72
3	Water	Et_3N[d]	100	0.2	5	80
4	**Water**	**K_2CO_3**	**100**	**0.2**	**4**	**85**
5	Water	K_2CO_3	80	0.3	5	78
6	Water	K_2CO_3	rt	0.3	24	25[e]

[a]Reaction of 4-Iodo anisole(1 mmol), methyl acrylate (2 mmol), Pd loading (0.2 mol%), K_2CO_3 (1 mmol), TBAB (10 mol%), water 3 mL.

[b]Isolated yields.

[c]Solvent was DMF.

[d]Triethyl amine was used as base.

[e]Room temperature.

Table II.B.4. Reaction of aryl halides with different vinyl compounds[a]

Entry	Aryl halides	Olefins	Product	Time (h)	Yield (%)[b]

1	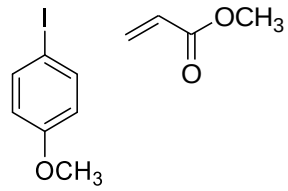		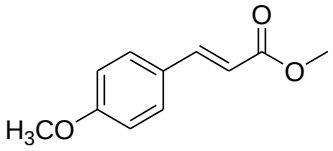	4	85
2	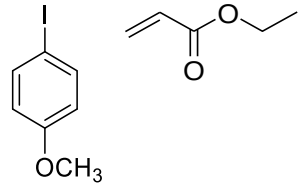		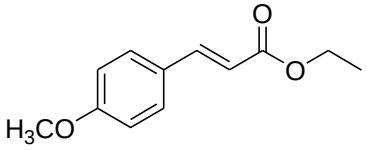	4	83
3	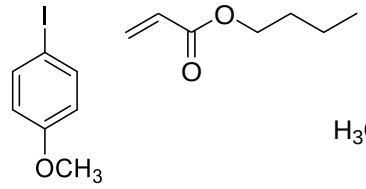		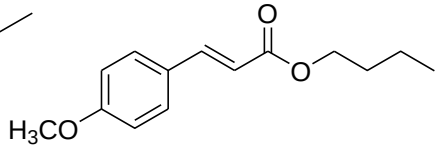	6	84
4	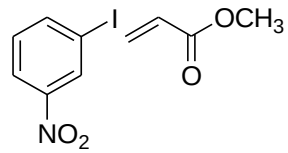		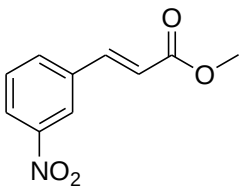	4	88
5	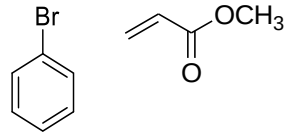		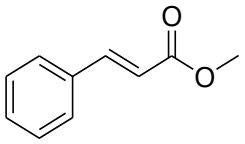	5	90
6	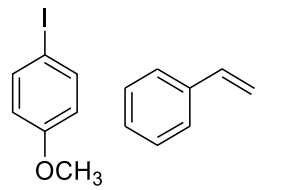		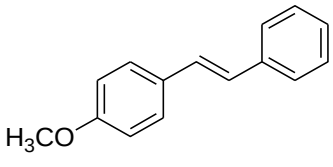	5	79

7	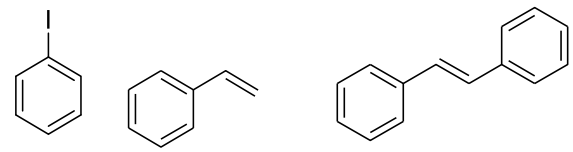		4	80
8	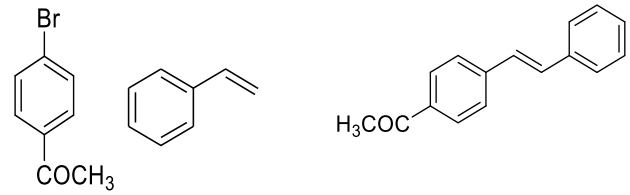		4	84

[a]Reaction of aryl halide (1 mmol), vinyl compound (2 mmol), GO-PMMA-Pd catalyst (0.2 mol%), K_2CO3 (1 mmol), TBAB (10 mol%), water 3 mL.

[b]Isolated yields.

The reduction of yield after 5th run of Suzuki coupling reaction (Figure II.B.6) could be due to the leaching of Pd NPs from GO-PMMA surface. The palladium content after 5th run was confirmed by ICP-AES and it was found to be 1.357 wt%. However, when the reaction was performed with only PMMA-Pd^0, a drastic change in yield was observed from 88% to 56% in 2nd run. This observation clearly indicated that presence of GO in the composite plays a vital role to improve the catalytic ability of GO-PMMA-Pd system.

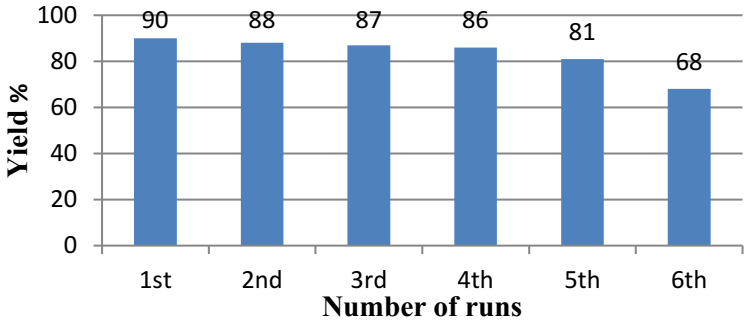

Figure II.B.6. *Recycling efficiencies of GO-PMMA-Pd catalyst for Suzuki coupling reaction.*

Leaching of metal from the heterogeneous GO-PMMA support was examined by hot filtration test as described in the literature [44]. After 1 h completion of reaction, the reaction mixture was filtered to separate out the catalyst and HPLC was carried out with the obtained filtrate (38 % conversion). The ICP-AES analysis of the filtrate showed the absence of any palladium. The filtrate was then heated for another 4 hrs at 90 ^{o}C without the addition of catalyst and the corresponding HPLC pattern did not show any noticeable conversion which implied that metals are not getting leached from the solid GO-PMMA support during 1st 1 h of the reaction (Figure II.B.7).

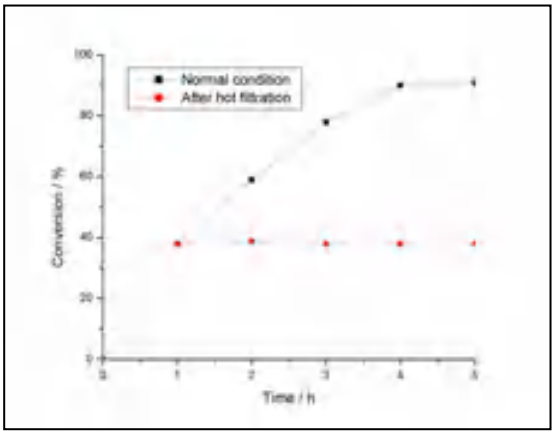

Figure II.B.7. *Comparison of normal time profile with hot filtration test. Conversions (±2%) at different time intervals for each plot were measured by HPLC.*

The Pd content was found to be 5.559 wt% in this heterogeneous catalyst. The recyclability of the catalyst was tested for Suzuki coupling reaction and the catalyst was recyclable for five consecutive runs without significant drop in activity. The sudden drop in yield (Figure II.B.6.) after the fifth run may be attributed to the leaching of Pd from the catalyst.

II.B.4. Conclusion

A greener protocol using ligand free GO-PMMA-Pd catalyst is proposed. The prepared catalyst was characterized by different spectroscopic and microscopic techniques. The newly made catalyst effectively generates different C-C cross coupled product even at a very low Pd content in high yields at optimal condition. The simple operational procedure, easy removal of catalyst, reusability of the catalyst and environmentally benign process are the most significant and outwit factors of our proposed scheme in comparison to the existing protocols.

II.B.5. Experimental Section

II.B.5.1. General Information

Palladium (II) acetate 99.98% was purchased from Sigma Aldrich. Graphite powder, H_2O_2 (solution 30%), 98.5% pure methyl methacrylate were purchased from commercial supplier. The morphology of the catalyst (GO-PMMA-Pd) was analyzed by Transmission Electron Microscope (TEM, Model: JEM-2100, accelerating voltages 60-200 KV in 50 V steps; resolution: 1.9Å to 1.4Å). Inductively coupled plasma spectroscopy (ICP) was analysed on ARCOS, Simultaneous ICP spectrometer (SPECTRO analytical instruments GmbH, Germany). Powder XRD data and X-ray photoelectron spectroscopy (XPS) was obtained from Bruker D8 Advanced X-ray Powder Diffractometer (Cu Kα radiation, λ = 1.54 Å) and an XPS instrument (Omicron: Serial no. 0571). NMR spectra were taken in $CDCl_3$ using a Bruker AV–300 spectrometer operating for ^1H at 300 MHz and for ^{13}C at 75 MHz. Splitting patterns of protons were described as s (singlet), d (doublet), t (triplet), br (broad) and m (multiplet).

Chemical shifts were reported in parts per million (ppm) relative to TMS as internal standard.

II.B.5.2. Procedure for cross coupling of 4-iodo anisole and phenyl boronic acid using GO-PMMA-Pd catalyst

A 25 mL RB was charged with 4-iodo anisole (1.0 mmol), phenylboronic acid (1.5 mmol), GO-PMMA-Pd catalyst (0.3 mol % Pd), K_2CO_3 (1 mmol), TBAB (10 mol %) and 2 mL water. The mixture was allowed to stir at 90 oC for an appropriate time (Table II.B.1) and the extent of the reaction was monitored by thin layer chromatography (TLC). After the completion of the reaction, the reaction mixture was extracted by ethyl acetate (2×25 ml) and washed with water repeatedly. The catalyst was filtered off and washed several times with ether and water (1:1) until no significant product was obtained in the wash. The recovered catalyst was reused for the next coupling experiment. The reaction mixture was dried over anhydrous Na_2SO_4, concentrated in vacuum and purified by column chromatography on silica gel 60-120 mesh using petroleum ether as eluent to obtain pure product. The catalyst recovered after 5th run was subjected to ICP-AES for Pd content analysis. The isolated products were analysed by ^1H NMR and ^{13}C NMR spectroscopy.

II.B.5.3. General procedures for the Heck coupling reactions

A mixture of 4-iodo anisole (1 mmol), methyl acrylate (2 mmol), GO-PMMA-Pd catalyst (0.2 mol % Pd), K_2CO_3 (1 mmol), TBAB (10 mol %) and 3ml water was stirred under 100 ^oC. The reaction took significant time for completion (Table II.B.3) and the progress of the reaction was monitored by TLC. After completion, the reaction mixture was extracted with ethyl acetate and washed with water repeatedly. The combined organic mixture was dried over anhydrous

Na_2SO_4 and purified by column chromatography using petroleum ether/ethyl acetate as eluent to afford pure product. The catalyst was separated and washed for several times with ether and water. The recovered catalyst was used in next cycles and the isolated products were characterized by ^1H and ^{13}C NMR spectroscopy.

II.B.5.4. Spectroscopic data of the products

4-methoxy-1,1′ biphenyl (Table II.B.2, entry 1) [45, 46]

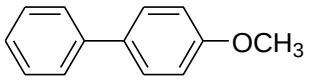

^1H NMR (300 MHz, $CDCl_3$) δ (ppm) 3.85 (s, 3H), 6.98 (d, 2H, *J* = 6.9 Hz), 7.24-7.32 (1H, m), 7.39 (d, 2H, *J* = 7.8Hz), 7.51-7.56 (m, 4H, *J* = 8.7 Hz);

^{13}C NMR (75 MHz, $CDCl_3$) δ (ppm) 55.37, 114.22, 126.68, 126.76, 128.18, 128.75, 133.80, 140.85,159.16.

3-methoxy-1,1′-biphenyl (Table II.B.2, entry 2) [45, 46]

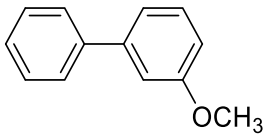

^1H NMR (300 MHz, $CDCl_3$) δ (ppm) 3.84 (s, 3H), 6.89 (d, *J* = 8.1 Hz, 1H), 7.12-7.18 (m, 2H), 7.31-7.36 (m, 2H), 7.39-7.44 (m, 2H), 7.58 (d, *J* = 8.1 Hz, 2H);

^{13}C NMR (75 MHz, $CDCl_3$) δ (ppm) 55.33, 112.72, 112.95, 119.74, 127.25, 127.47, 128.79, 129.81, 141.15, 142.82, 159.89.

3-nitro-1,1'-biphenyl (Table II.B.2, entry 3) [45, 46]

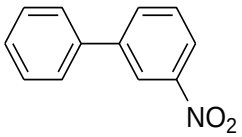

^{1}H NMR ($CDCl_3$, 300MHz) δ 8.41 (s, 1H), 8.15 (s,1H), 7.87 (s,1H), 7.41-7.59 (m, 7H, *J* = 8.4Hz);

^{13}C NMR (75 MHz, $CDCl_3$) δ (ppm) 121.93, 122.04, 127.17, 128.58, 129.20, 129.70, 133.06, 138.65, 142.86, 148.74.

4-methyl-1,1′-biphenyl (Table II.B.2, entry 4) [45, 46]

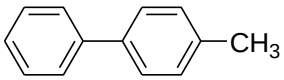

^{1}H NMR (300 MHz, $CDCl_3$) δ (ppm) 2.174 (s, 3H), 6.95-6.99 (d, 2H, *J* = 6.9Hz), 7.23-7.31(m, 1H), 7.38-7.51 (m, 2H), 7.52-7.56 (q, 4H);

^{13}C NMR (75 MHz, $CDCl_3$) δ (ppm) 21.12, 122.00, 127.01, 128.74, 129.20, 129.50, 133.07.

3-methyl 1,1'-biphenyl (Table II.B.2, entry 5) [52]

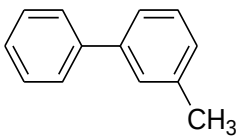

^{1}H NMR (300 MHz, $CDCl_3$) δ (ppm) 2.39 (s, 3H), 6.88 (d, *J* = 8.1Hz, 1H), 7.13-7.19(m, 2H), 7.31-7.36 (m, 2H), 7.42-7.44 (m, 2H), 7.59 (d, *J* = 8.1Hz, 2H);

^{13}C NMR (75 MHz, $CDCl_3$) δ (ppm) 26.68, 124.30, 127.20, 127.28, 128.02, 128.69, 128.78, 138.35, 141.26, 141.37.

4-acetyl 1,1'-biphenyl (Table II.B.2, entry 6) [47]

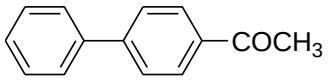

^{1}H NMR (300 MHz, $CDCl_3$) δ (ppm) 2.68 (s, 3H), 7.39-7.49 (m, 3H, *J* = 7.5Hz), 7.61-7.68 (m, 4H, *J* = 7.2Hz), 8.00 (d, 2H, *J* = 8.1Hz);

^{13}C NMR (75 MHz, $CDCl_3$) δ (ppm) 26.68, 127.24, 127.29, 128.26, 128.94, 128.98, 135.86, 139.87, 145.79, 197.80.

4-methoxy-3-methyl-1,1'-biphenyl (Table II.B.2, entry 7) [47]

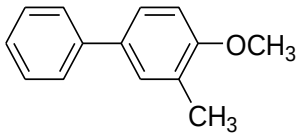

^{1}H NMR (300 MHz, $CDCl_3$) δ (ppm) 2.28 (s, 3H), 3.86 (s, 3H), 7.17 (s, 1H), 6.81(s, 1H), 7.39 (t, 4H), 7.55 (t, 2H);

^{13}C NMR (75 MHz, $CDCl_3$) δ (ppm) 16.43, 55.45, 110.17, 126.40, 126.55, 126.78, 126.91, 128.69, 129.52, 133.36, 141.07, 157.39.

4-methyl-4'-methoxy-1,1'-biphenyl (Table II.B.2, entry 9) [45, 47]

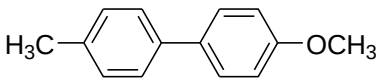

^{1}H NMR (300 MHz, $CDCl_3$) δ (ppm) 2.39 (s,3H), 3.84 (s, 3H), 6.97 (d, 2H, *J* =7.5Hz), 7.23 (d, 2H, *J* = 8.4Hz), 7.44-7.55 (m, 4H);

^{13}C NMR (75 MHz, $CDCl_3$) δ (ppm) 24.25, 58.52, 117.34, 129.77, 131.14, 132.64, 136.92, 139.55, 141.14, 162.10.

2-phenylthiophene (Table II.B.2, entry 10) [46, 47]

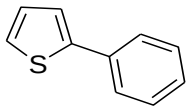

^{13}C NMR (75 MHz, $CDCl_3$) δ (ppm) 118.98, 126.24, 127.97, 129.06, 130.63, 131.21, 132.06, 137.51.

(*E*)-methyl 3-(3-nitrophenyl) acrylate (Table II.B.4, entry 4) [50]

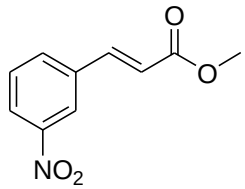

^{1}H NMR (300 MHz, $CDCl_3$) δ (ppm) 3.84 (s, 3H), 6.57 (d, *J* = 15.9 Hz), 7.57-7.84 (m, 3H), 8.24 (d, 1H, *J* = 8.1 Hz), 8.38 (s, 1H);

^{13}C NMR (75 MHz, $CDCl_3$) δ (ppm) 55.18, 124.10, 125.58, 127.70, 133.12, 136.78, 139.24, 145.12, 151.81, 169.73.

(*E*)-methyl 3-(4-methoxyphenyl) acrylate (Table II.B.4, entry 1) [49]

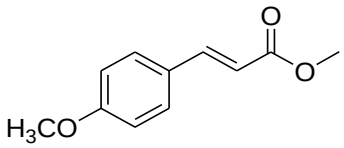

^{1}H NMR (300 MHz, $CDCl_3$) δ (ppm) 3.68 (s, 1H), 3.77 (s, 1H), 6.47 (d, 1H, *J* = 15.9Hz), 6.95 (d, 2H, *J* = 8.7Hz), 7.65 (d, 3H, *J* = 8.8Hz);

^{13}C NMR (75 MHz, $CDCl_3$) δ (ppm) 51.27, 55.29, 114.33, 115.03, 126.57, 130.13, 144.31, 161.11, 166.91.

(*E*)-ethyl 3-(4-methoxyphenyl) acrylate (Table II.B.4, entry 2) [47, 49]

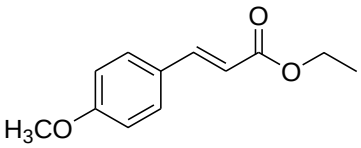

^{1}H NMR ($CDCl_3$, 300 MHz) δ 0.98-1.02 (t, 3H), 3.47 (s, 1H), 4.13-4.17 (q, 2H), 6.43 (d, 1H, *J* =16.2 Hz), 6.92-6.95 (d, 2H, *J* = 8.4Hz), 7.58-7.62 (m,3H);

^{13}C NMR (75 MHz, $CDCl_3$) δ (ppm) 14.06, 55.08, 59.71, 114.21, 115.30, 116.53, 126.58, 129.92, 137.84, 144.00, 161.04, 166.39.

(*E*)-butyl 3-(4-methoxyphenyl) acrylate (Table II.B.4, entry 3) [51]

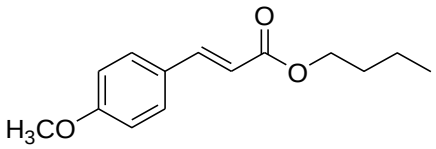

^{1}H NMR (300 MHz, $CDCl_3$) δ (ppm) 1.00 (t, 3H, *J* = 6.6Hz), 1.44 (m, 2H), 1.69 (m, 2H), 3.80 (s, 3H), 4.16-4.23 (t, 2H, *J* = 6.6Hz), 6.89 (2H, d, *J* = 8.7Hz), 7.63 (d, 1H, *J* = 16.2Hz), 7.47 (t, 3H);

^{13}C NMR (75 MHz, $CDCl_3$) δ (ppm) 16.90, 22.35, 33.96, 58.43, 67.37, 117.42, 118.85, 130.30, 132.81, 147.34, 164.46, 170.54.

1-(4-styrylphenyl)ethanone (Table II.B.4, entry 8) [47]

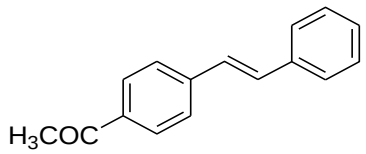

^{1}H NMR (300 MHz, $CDCl_3$) δ (ppm) 2.55 (s, 3H), 7.08-7.19 (m, 2H), 7.21 (d, 1H, *J* = 16.8Hz), 7.29-7.58 (m, 5H), 7.97 (d, 2H, *J* = 8.4Hz);

^{13}C NMR (75 MHz, $CDCl_3$) δ (ppm) 29.79, 129.70, 130.02, 130.62, 131.52, 132.00, 132.08, 134.65, 139.12, 139.87, 145.19, 200.71.

II.B.5.5. Scanned copies of ^{1}H and ^{13}C NMR spectra of synthesised compounds.

Figure II.B.8. *Scanned copy of ^{1}H and ^{13}C NMR spectra of 4-methoxy-1,1′ biphenyl.l*

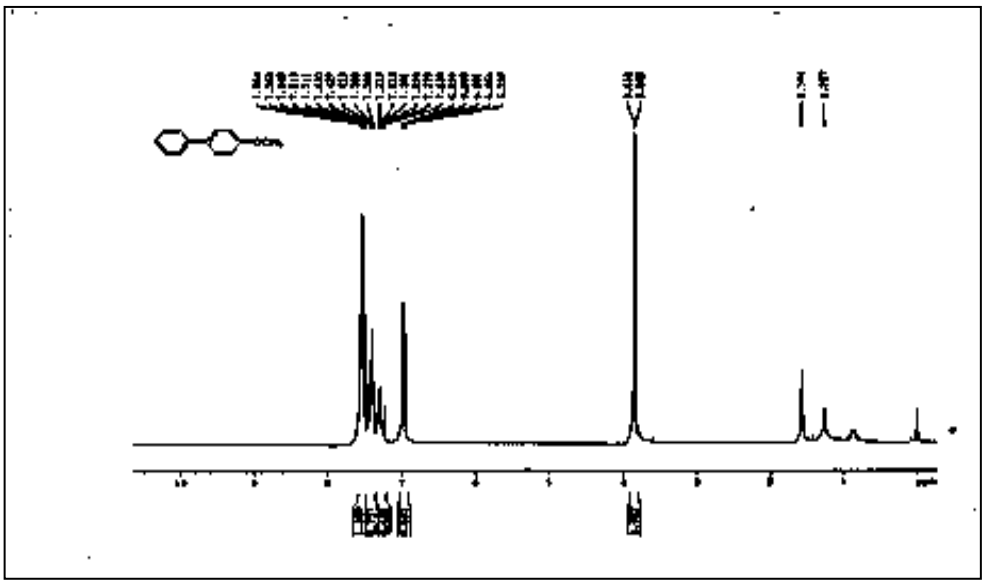

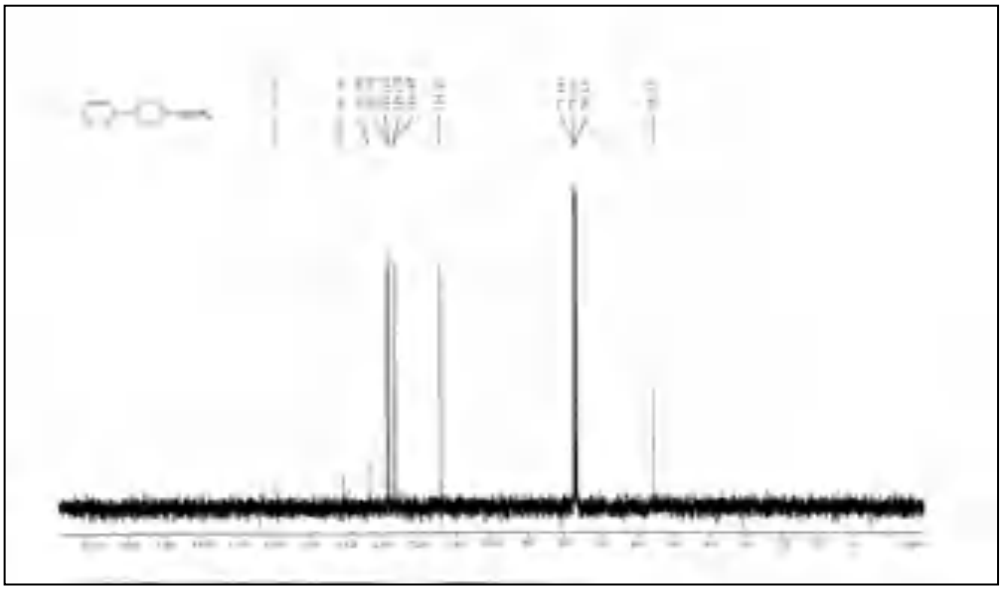

Figure II.B.9. *Scanned copy of ^{1}H and ^{13}C NMR spectra of 3-methoxy-1,1′-biphenyl.*

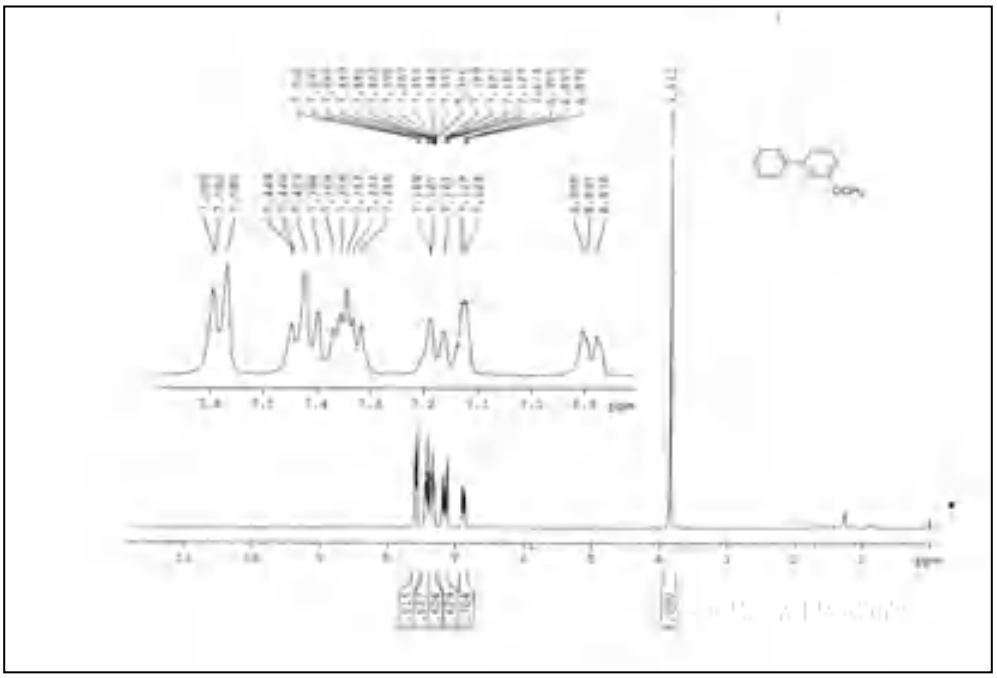

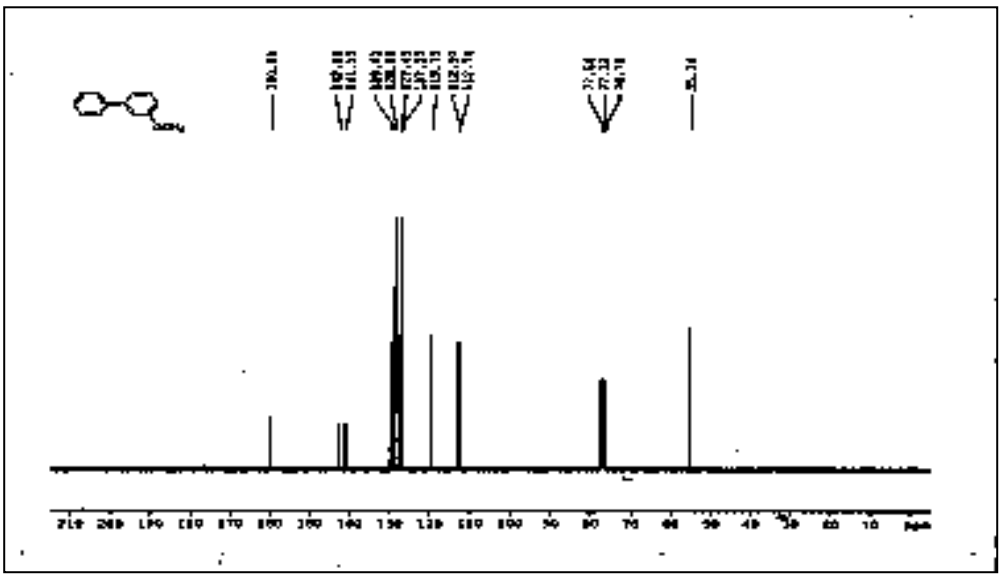

Figure II.B.10. *Scanned copy of ^{1}H and ^{13}C NMR spectra of 3-nitro-1,1'-biphenyl.*

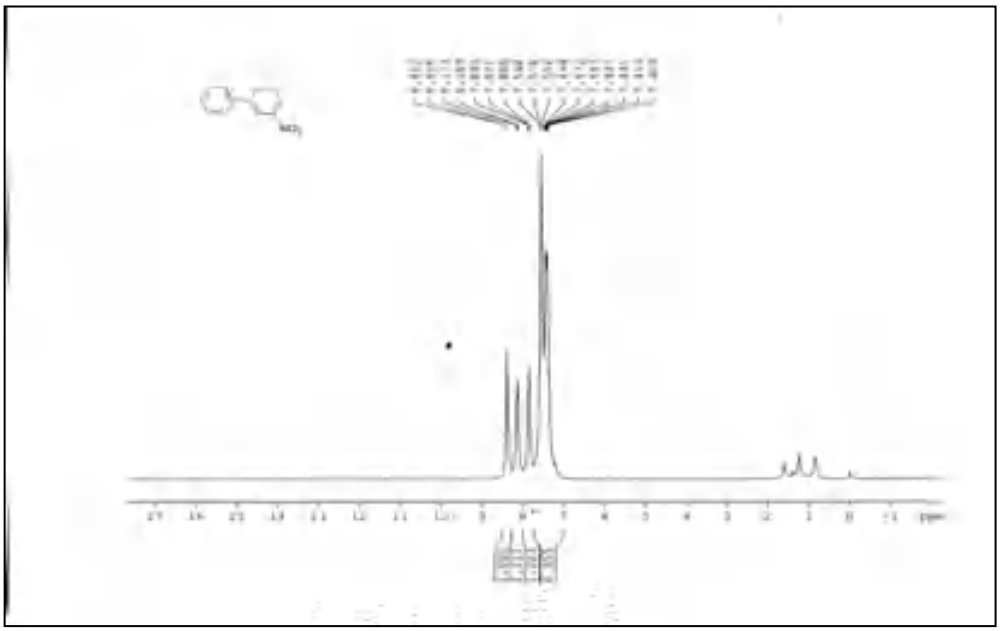

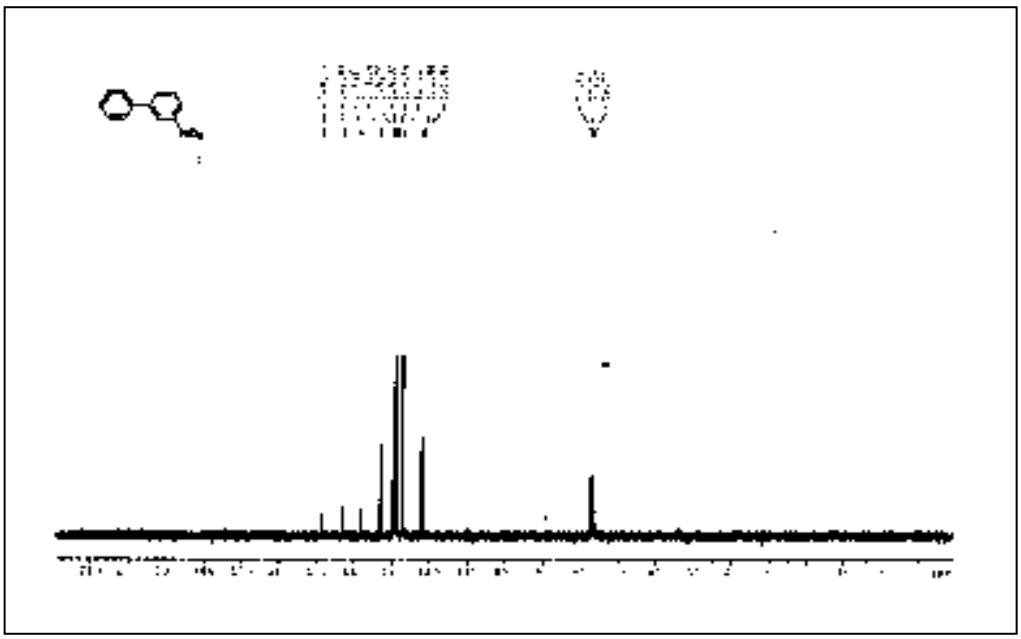

Figure II.B.11. *Scanned copy of ^{1}H and ^{13}C NMR spectra of 4-methyl-1,1′-biphenyl.*

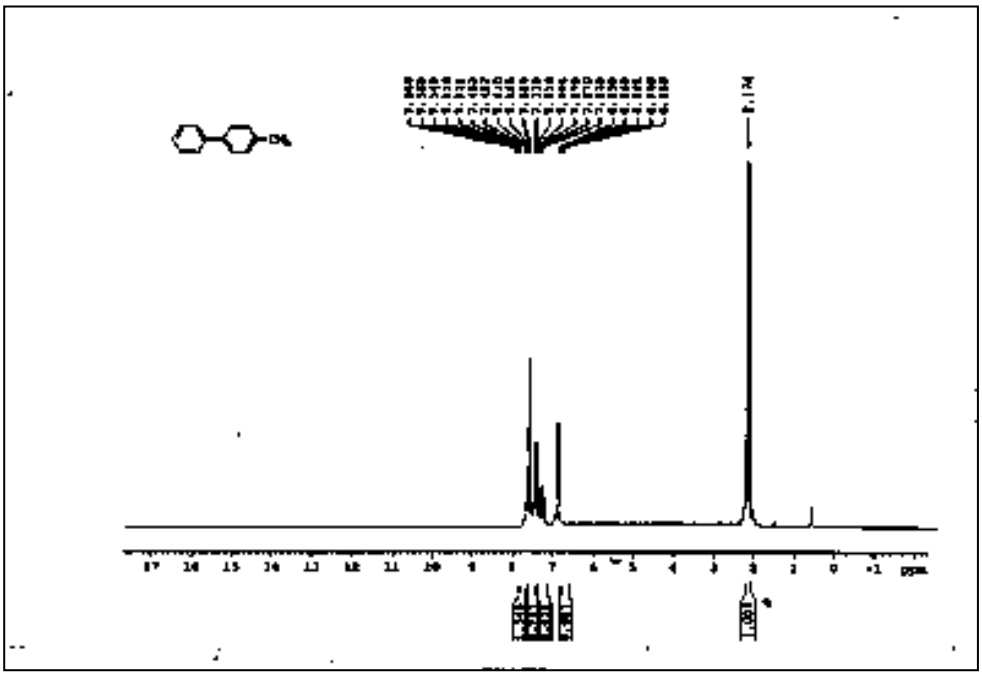

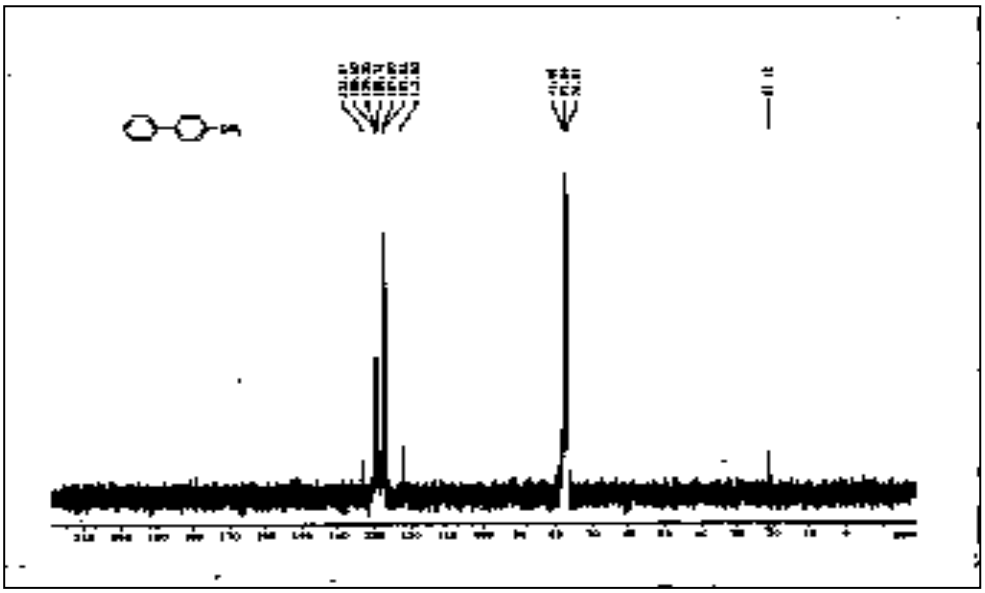

Figure II.B.12. *Scanned copy of ^{1}H and ^{13}C NMR spectra of 4-acetyl 1,1'-biphenyl.*

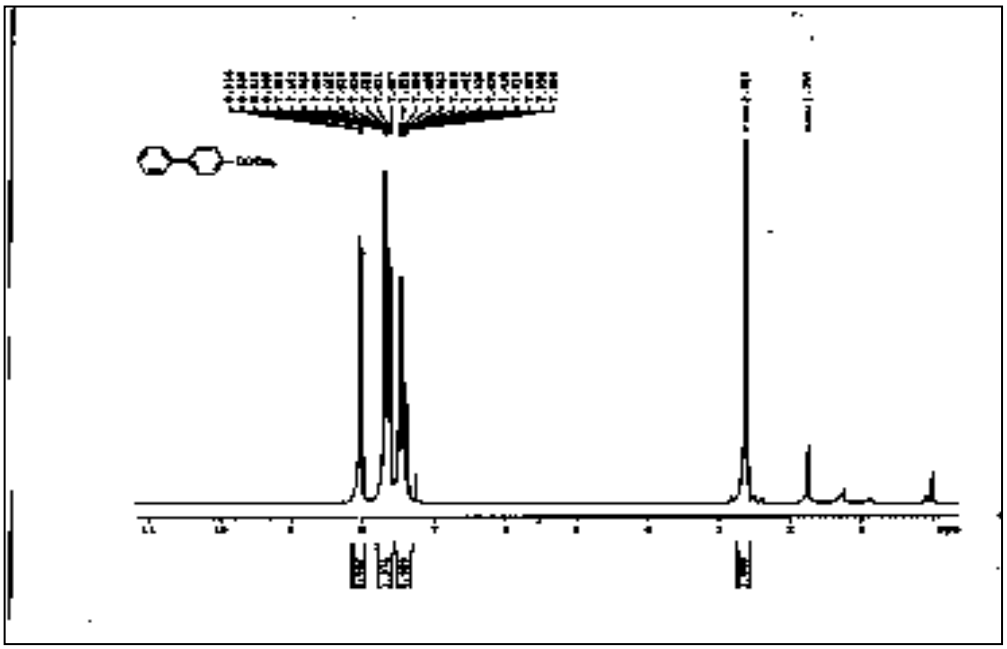

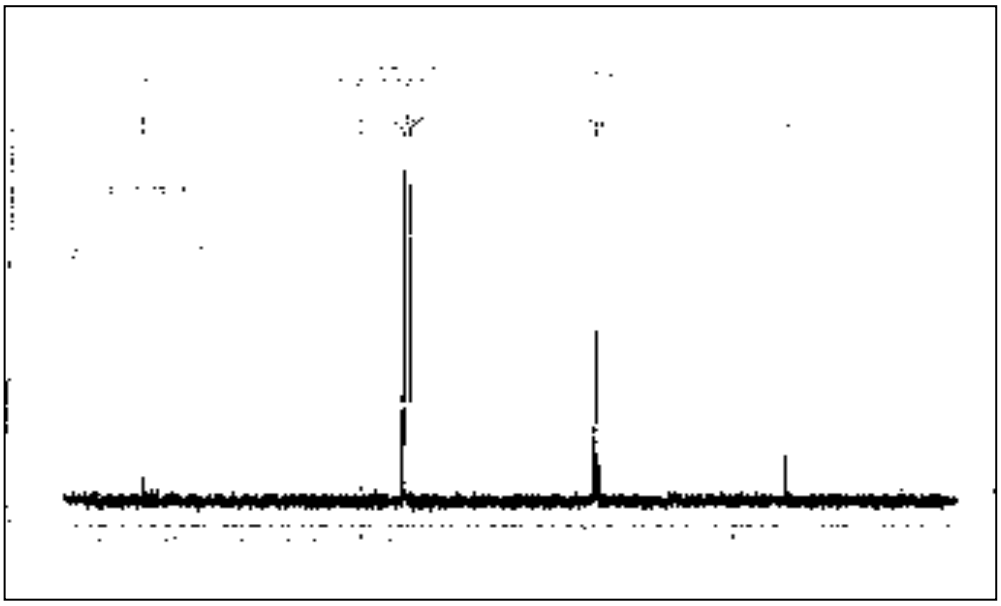

Figure II.B.13. *Scanned copy of ^{1}H and ^{13}C NMR spectra of 4-methoxy-3-methyl-1,1'-biphenyl.*

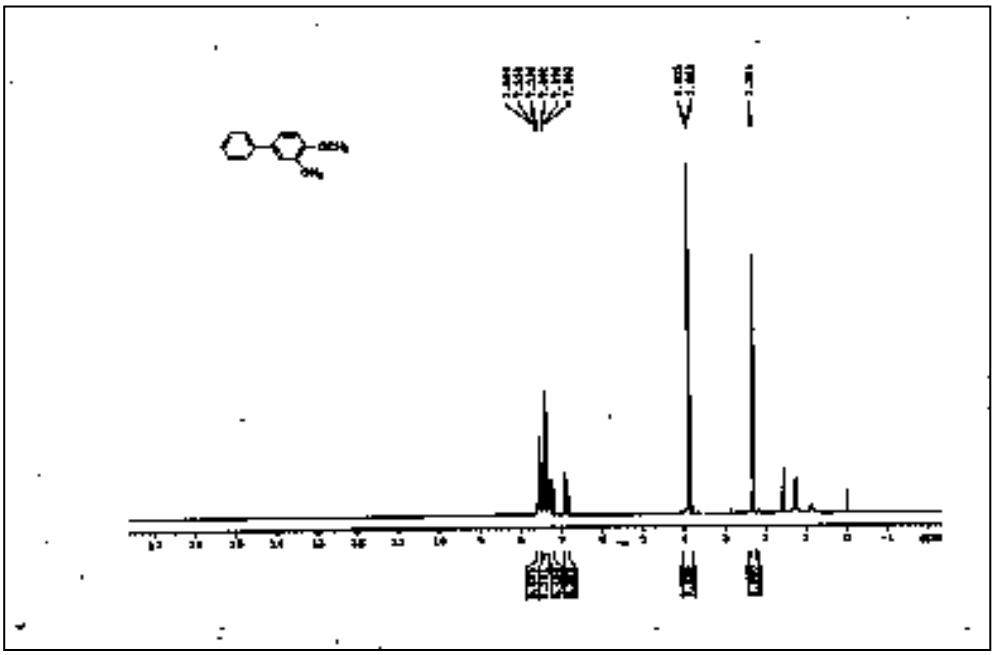

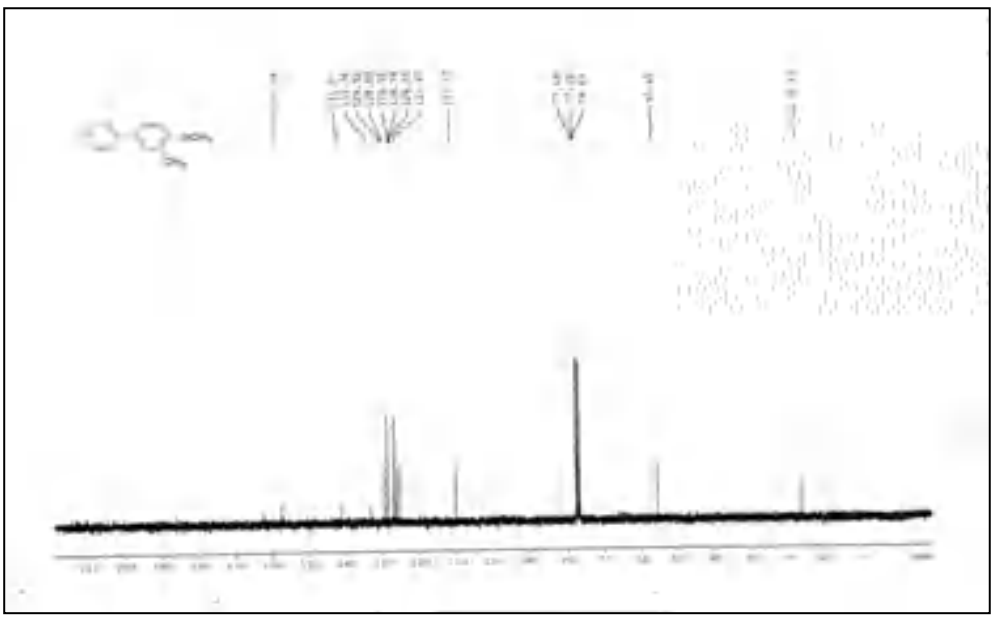

Figure II.B.14. *Scanned copy of ^{1}H and ^{13}C NMR spectra of 4-methyl-4'-methoxy-1,1'-biphenyl.*

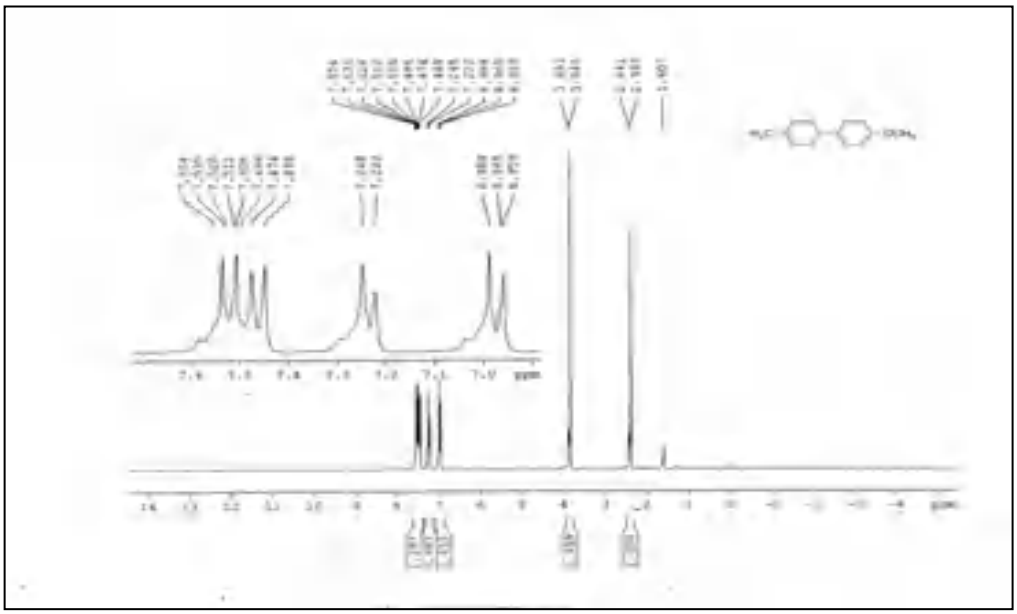

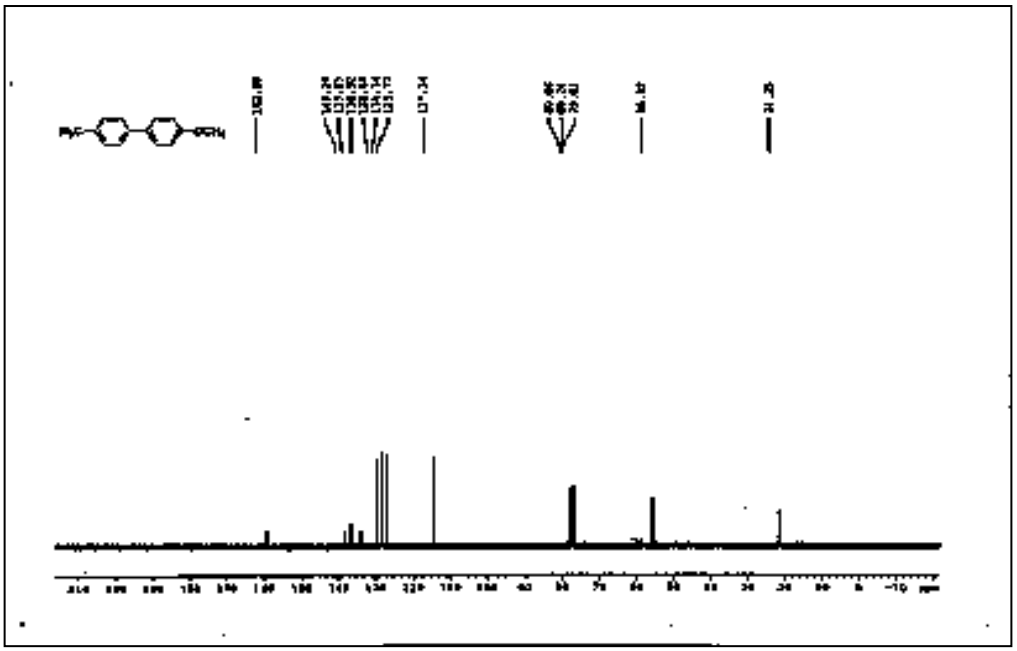

Figure II.B.15. *Scanned copy of ^{1}H and ^{13}C NMR spectra of (E)-methyl 3-(3-nitrophenyl)acrylate.*

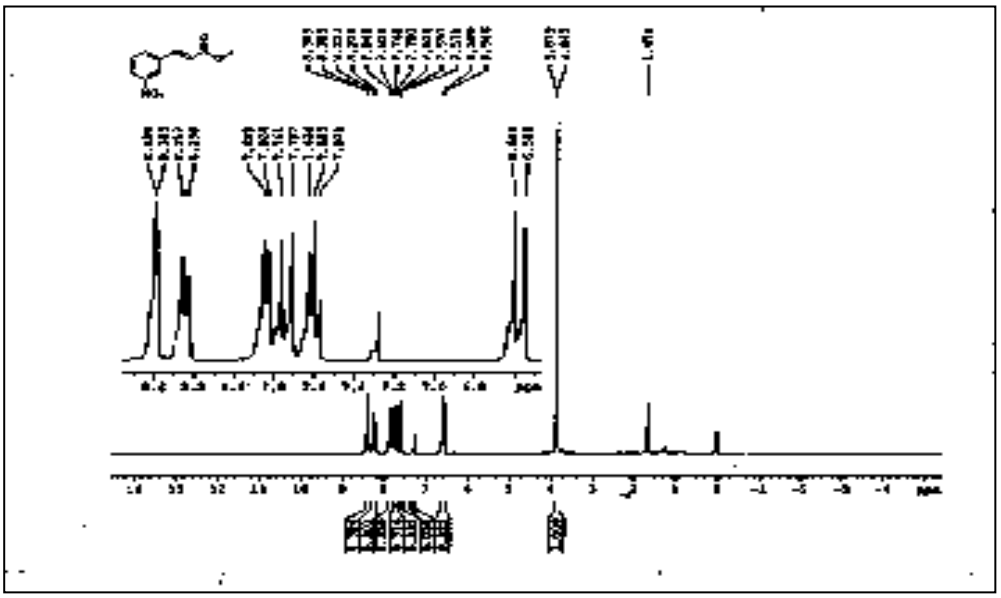

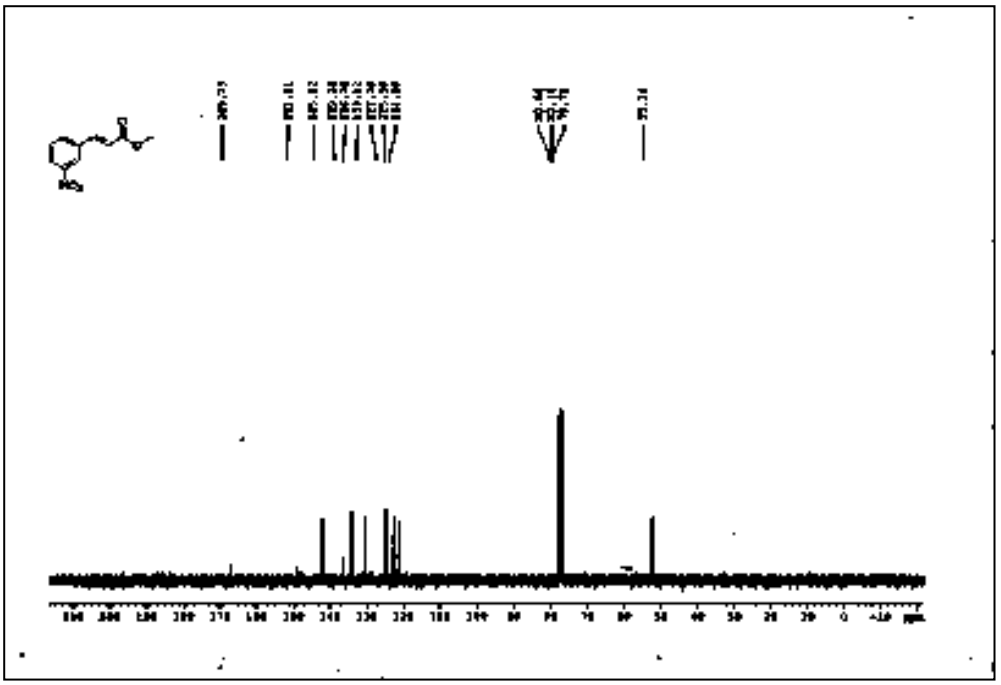

Figure II.B.16. *Scanned copy of ^{1}H and ^{13}C NMR spectra of (E)-methyl 3-(4-methoxyphenyl) acrylate.*

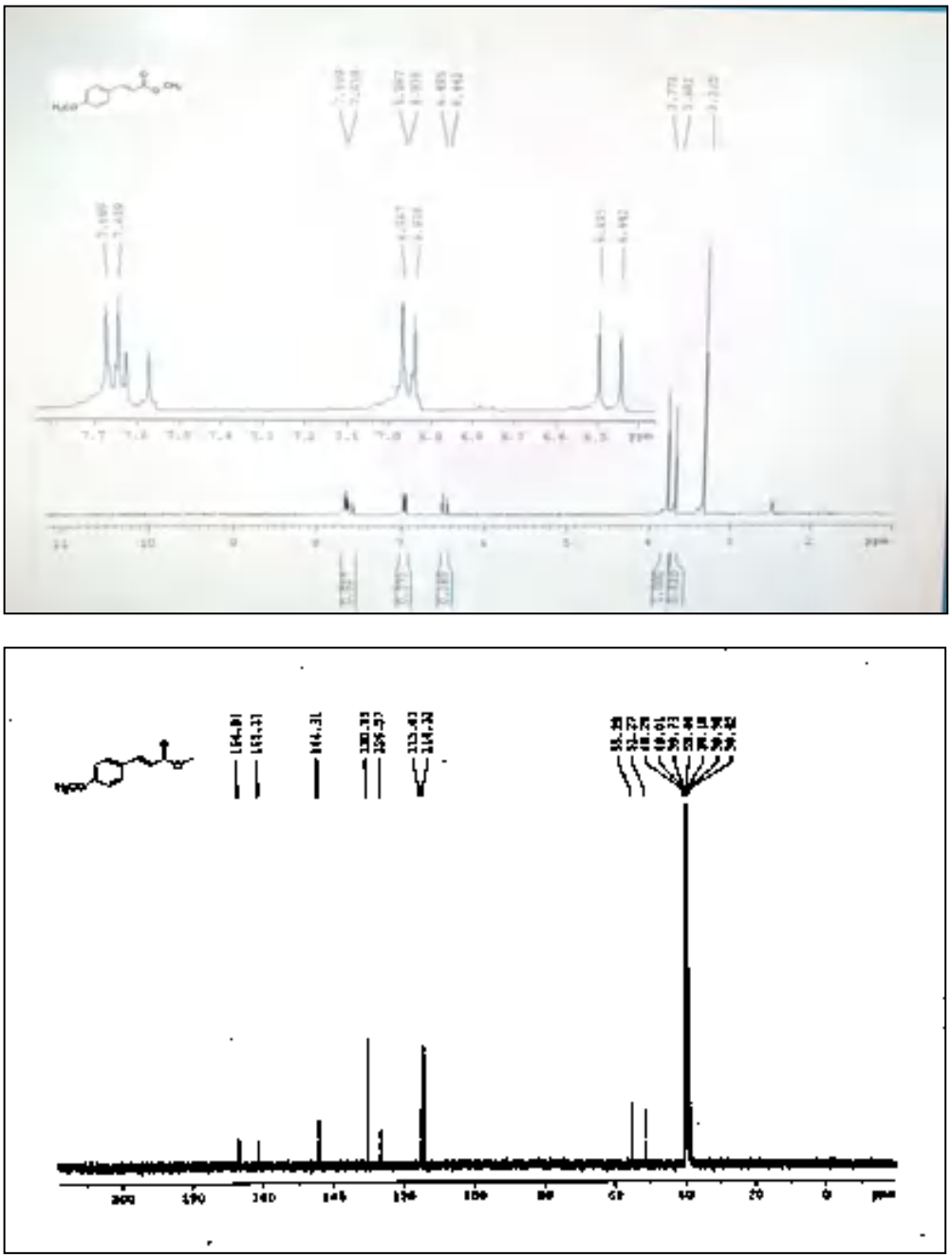

Figure II.B.17. *Scanned copy of ^{1}H and ^{13}C NMR spectra of (E)-ethyl 3-(4-methoxyphenyl) acrylate.*

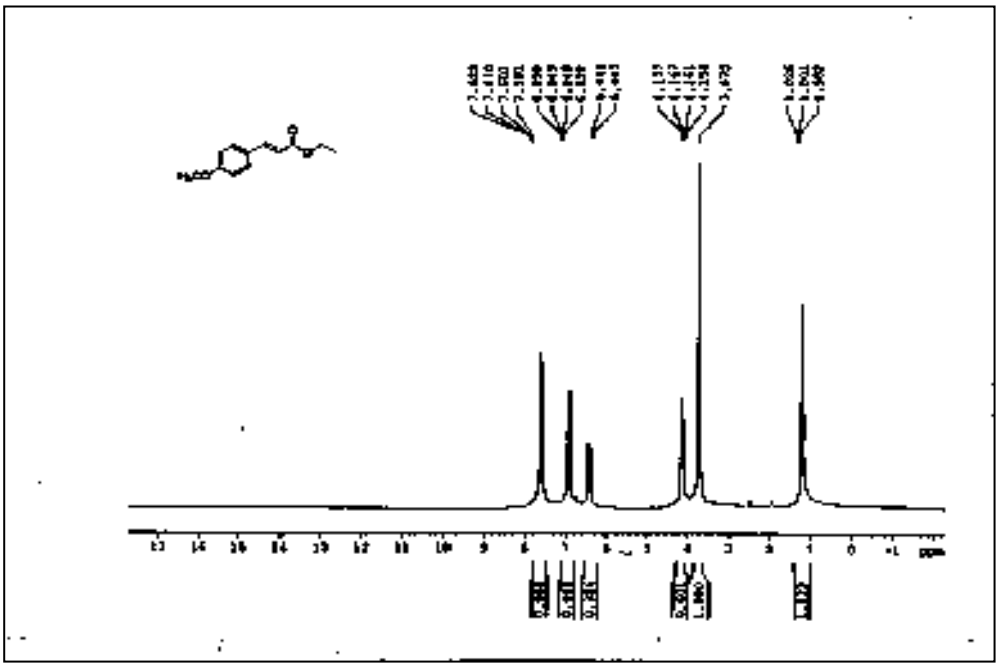

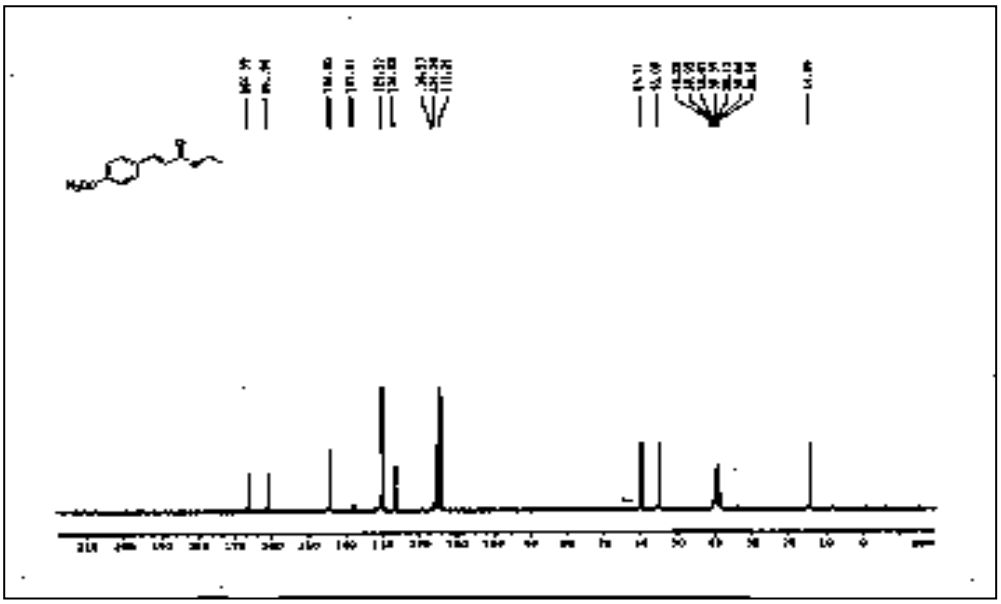

Figure II.B.18. *Scanned copy of ^{1}H and ^{13}C NMR spectra of (E)-butyl 3-(4-methoxyphenyl) acrylate.*

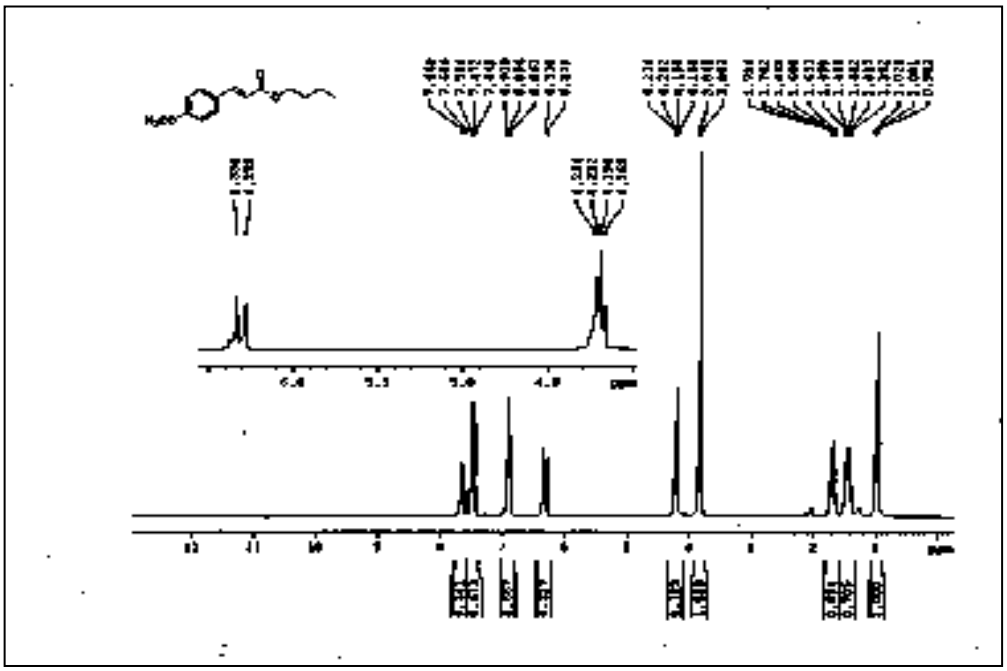

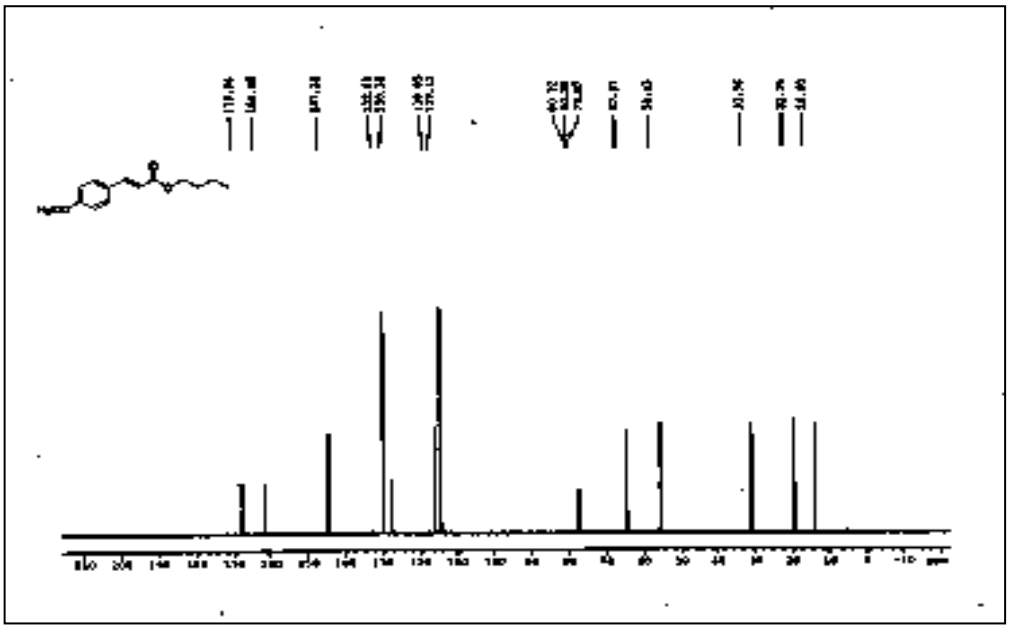

Figure II.B.19. *Scanned copy of ^{1}H and ^{13}C NMR spectra of 1-(4-styrylphenyl)ethanone.*

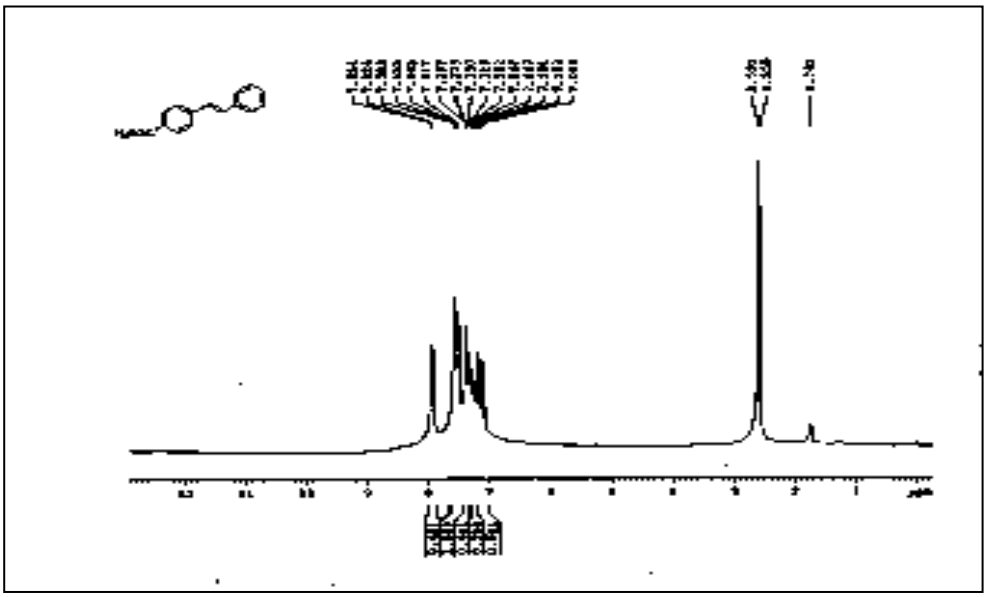

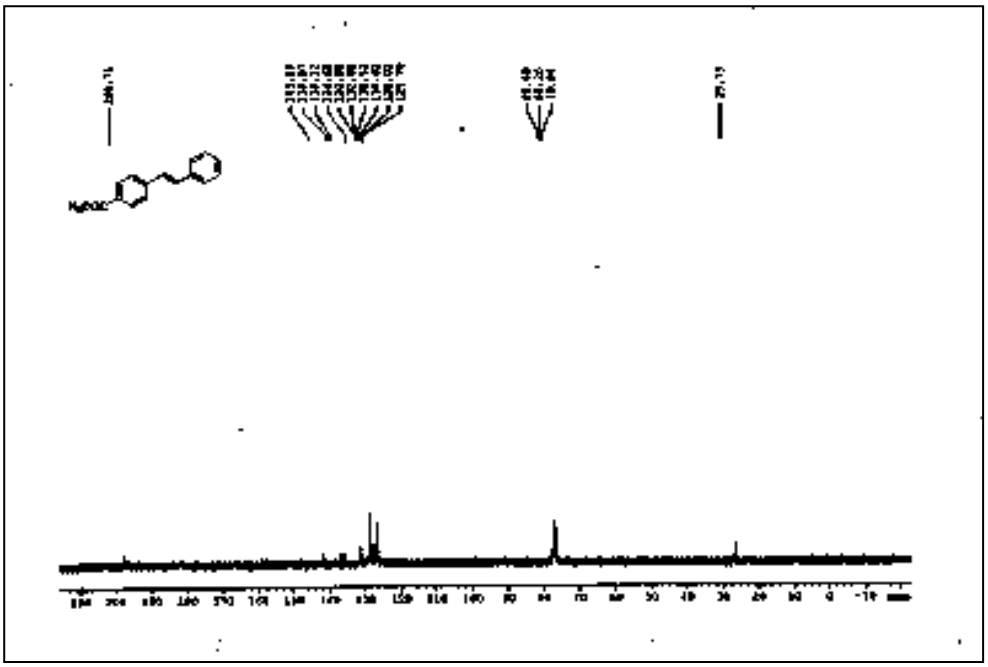

II.B.6. References

References are given in Bibliography under Chapter II, Section B